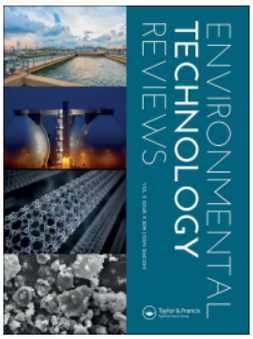

Environmental Technology Reviews

ISSN: 2162-2515 (Print) 2162-2523 (Online) Journal homepage: www.tandfonline.com/journals/tetr20

Advancements in thermal management of lithium-ion batteries: the role of nanofluids and phase change materials

Farhan Lafta Rashid, Mudhar A. Al-Obaidi, Najah M. L. Al Maimuri, Ali M. Ashour, Shabbir Ahmad, Arman Ameen, Saif Ali Kadhim, Karrar A. Hammoodi, Wisam J. Khudhayer & Ali Altaee

To cite this article: Farhan Lafta Rashid, Mudhar A. Al-Obaidi, Najah M. L. Al Maimuri, Ali M. Ashour, Shabbir Ahmad, Arman Ameen, Saif Ali Kadhim, Karrar A. Hammoodi, Wisam J. Khudhayer & Ali Altaee (2026) Advancements in thermal management of lithium-ion batteries: the role of nanofluids and phase change materials, Environmental Technology Reviews, 15:1, 40-75, DOI: 10.1080/21622515.2025.2609810

To link to this article: https://doi.org/10.1080/21622515.2025.2609810

Published online: 02 Jan 2026.

ENVIRONMENTAL TECHNOLOGY REVIEWS
2025, VOL. 15, NO. 1, 40–75
https://doi.org/10.1080/21622515.2025.2609810

Taylor & Francis
Taylor & Francis Group

REVIEW ARTICLE

OPEN ACCESS Check for updates

Advancements in thermal management of lithium-ion batteries: the role of nanofluids and phase change materials

Farhan Lafta Rashid [a], Mudhar A. Al-Obaidi [b], Najah M. L. Al Maimuri [c], Ali M. Ashour[d], Shabbir Ahmad [e,f], Arman Ameen [g], Saif Ali Kadhim[d], Karrar A. Hammoodi[h], Wisam J. Khudhayer[i] and Ali Altaee [j]

[a]Petroleum Engineering Department, College of Engineering, University of Kerbala, Karbala, Iraq; [b]Technical Instructor Training Institute, Middle Technical University, Baghdad, Iraq; [c]Building and Construction Techniques Engineering Department, College of Engineering and Engineering Techniques, Al-Mustaqbal University, Hillah, Iraq; [d]Mechanical Engineering Department, University of Technology- Iraq, Baghdad, Iraq; [e]Graduate Program of Ocean Engineering, School of Engineering, Universidade Federal do Rio Grande, Rio Grande, Brazil; [f]Institute of Geophysics and Geomatics, China University of Geosciences, Wuhan, People's Republic of China; [g]Department of Building Engineering, Energy Systems and Sustainability Science, University of Gävle, Gävle, Sweden; [h]College of Engineering, University of Al Maarif, Al Anbar, Iraq; [i]Department of Energy and Renewable Energies Engineering, College of Engineering / Al- Musayab, University of Babylon, Babylon, Iraq; [j]Centre for Green Technology, School of Civil and Environmental Engineering, University of Technology Sydney, Australia

ABSTRACT

This paper investigates the application of nanofluids in lithium-ion battery (LIB) thermal management through a comprehensive review of thermal management system (TMS) development. The review focuses on systems incorporating both phase change materials (PCMs) and nanofluid technologies as solutions for managing heat generation and thermal hazards in LIBs. It demonstrates that traditional cooling techniques, such as air and liquid cooling, are less effective than nanofluids. These colloidal suspensions of nanoparticles (e.g. Al_2O_3, CuO, TiO_2, AgO, as well as carbon-based nanomaterials) in base fluids enhance both thermal conductivity and convective heat transfer performance. The review demonstrats that using Al_2O_3-water nanofluids with a 2% volume fraction can reduce peak temperatures by 1.2°C, while hybrid nanofluids containing Al_2O_3-CuO can reduce temperatures by up to 54.23% at a 0.5% concentration. When PCMs are combined with nanofluids to form hybrid systems, maximum temperature reduction of up to 19.5% has been observed. These hybrid systems also contribute to greater thermal uniformity and delayed temperature increases. However, challenges such as nanoparticle stability, increased pressure drops, and environmental and economic concerns remain significant obstacles. This review concludes that TMSs using nanofluids in conjunction with PCMs within optimised channel designs show promising potential for enhancing LIB performance, though further research is needed to overcome the associated barriers.

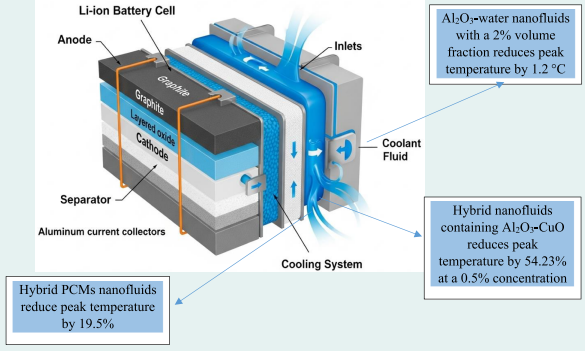

ARTICLE HISTORY
Received 24 April 2025
Accepted 18 December 2025

KEYWORDS
Thermal management; energy efficient; lithium-ion batteries (LIBs); nanofluid; phase change materials (PCMs)

Nomenclature

Symbol Definition

CFD	Computational Fluid Dynamics
CNT	Carbon nanotube
EV	Electric vehicles
FEM	Finite element method
HC-PHP	Helical coiled pulsing heat pipe

CONTACT Arman Ameen arman.ameen@hig.se Department of Building Engineering, Energy Systems and Sustainability Science, University of Gävle, Gävle 801 76, Sweden

LIBPs	Lithium-ion battery packs
LCOH	Levelized cost of hydrogen
LB	Lattice Boltzmann
Nf	Nanofluid
NMF	Nanoparticle mass fraction
NNfs	Non-Newtonian nanofluids
NPs	Nanoparticles
MCH	Helical microchannel
OHP	Hybrid oscillating heat pipe
PHP	Pulsing heat pipe
rGO	Reduced graphene oxide
THNF	Ternary hybrid nanofluids
VPNPs	Volume percentage of nanoparticles

1. Introduction

Lithium-ion battery (LIB) has become the foremost energy storage technology, extensively used across different domains – from portable electronics to electric vehicles (EV) and electricity grid storage applications. Several parameters can affect its market success, including high energy storage efficacy and the capacity to operate over many cycles with minimal natural power loss [1–3]. However, LIB systems now face thermal management as a serious challenge, predominantly as the request for higher energy density and faster charging continues to raise. Excessive heat generated during charging and discharging cycles shortens battery lifespan and accelerates wear, while thermal runaway – a condition where heat generation becomes uncontrollable – poses catastrophic risks to the device [4]. The thermal performance of LIB is specifically impacted by a number of parameters, including operating speed, environmental conditions, and electrical resistance [5]. Heat is produced during operation via Joule heating, entropic heating, and electrochemical reactions. This accumulated heat can increase battery temperatures further than the safe operating range, classically between 15°C and 35°C [6,7].

Among the most highlighted concerns is thermal runaway, that happens when exothermic reactions within the battery produce heat faster than it can be dissipated to the external environment [8]. Zhang et al. [9] utilised a thorough modelling to specify key safety thresholds for thermal runaway, emphasising the significance of robust thermal management systems (TMS). Different strategies are presented to protect LIBs through thermal management, including air cooling, liquid cooling, PCMs, and hybrid solutions [10]. Air cooling, though economically simple, often delivers inadequate thermal regulation for high-power implications. However, liquid cooling delivers greater heat transfer performance but comprises more complicated systems, such as pumps and heat exchangers, besides the risk of fluid leakage. Lai et al. [11] established a compact liquid-cooled thermodynamic system for cylindrical batteries, that attained expressively better temperature uniformity than conventional air cooling systems. Recent progressions in the field of thermal management have motivated on the design of ground-breaking cooling plates. Mo et al. [12] engaged topology optimisation to design cooling plates, which simultaneously advance both temperature uniformity and pressure drop. This technique presented improved liquid cooling capabilities, optimising heat hotspot mitigation and overall energy usage. Zhao et al. [13] optimised liquid-cooled plate structures for EV, representing that simple shape changes can meaningfully boost performance while preserving system simplicity.

Nanofluids have incorporated as an pioneering solution that improves conventional liquid cooling systems. These fluids, composed of nanoparticles (NPs) dispersed in base fluids, deliver greater thermal properties by improving thermal conductivity and upgrading convective heat transfer in a comparison to traditional coolants [14]. Zhong et al. [15] examined ferro-nanofluid flow within porous microchannels and established that the use of magnetic fields would considerably enhance the heat transfer. This investigation assigned the potential of magnetic-field-responsive nanofluids to function in dynamic TMSs that adapt to various heat loads under a wide set of operating conditions.

The employment of nanofluids in battery thermal management systems would enable modern battery technologies to resolve escalating thermal challenges. In this aspect, Kanti et al. [16] directed an experimental investigation using machine learning techniques to assess the success of both hybrid and mono nanofluids in LIB cooling. The results indicated that strategically designed hybrid nanofluids can outperform single nanofluids and conventional coolants, putting them as favourable thermal management solutions for the future. Nanofluids also complement PCMs, that excellently manage heat through their phase transition mechanisms. Cai et al. [17] presented a new method by mixing Ti_3C_2Tz MXene material into the anode, permitting built-in thermal protection while signifying potential for integrated battery material thermal control. This pioneering development combines thermal management tactics with battery material design protocols, outstanding the restrictions of separate external cooling systems.

The challenge of thermal management extends beyond simply preventing thermal runaway; it also involves maintaining optimal temperatures for performance and preserving battery lifespan. Chen et al. [18] investigated battery structural deformation and safety risks caused by thermal radiation, emphasising the

critical importance of multi-mode heat transfer management in achieving fully effective thermal strategies for batteries. Napa et al. [19] developed an electro-thermal model to demonstrate how prismatic cells should be managed during EV drive cycles, where dynamically changing thermal demands are present. The advancement of BTMS is becoming increasingly linked to improved computational modelling and machine learning applications. Li et al. [20] constructed a digital twin system using CNN-LSTM-attention networks for real-time degradation forecasting, enabling the use of thermal data for predictive maintenance and system optimisation. Yao et al. [21] demonstrated the potential of semi-supervised adversarial deep learning for evaluating battery energy storage system capacity – an emerging approach in battery management technologies.

Recent research has also highlighted the effectiveness of innovative cooling channel designs. Bahrami et al. [22] studied novel spiral micromixers featuring sinusoidal channel geometries and analyzed their performance under non-uniform magnetic fields for enhanced mixing. Their findings on geometric optimisation and external field manipulation for improved heat transfer are directly applicable to next-generation battery cooling systems, even though their work focused on non-battery applications. In a comprehensive review, Sun et al. [23], analysed photo-rechargeable lithium and zinc-ion batteries, highlighting the unique thermal management requirements of these emerging battery chemistries. Additionally, Xiang et al. [24] emphasised the need for detailed economic evaluations of various energy storage technologies, as thermal regulation significantly influences the levelized cost of hydrogen (LCOH) in electrolysis systems. Gasmelseed et al. [25] conducted an extensive review of research on nanofluid-based BTMS. Nanofluids showed significant potential as coolants due to their enhanced thermal conductivity, which allows them to outperform conventional fluid coolants. The aforementioned reviewed studies investigated various nanoparticle types, including copper oxide (CuO), aluminum oxide (Al_2O_3), and silver oxide (AgO), at concentrations ranging from 0.1% to 5%. However, the literature review highlighted the need for further research into the durability of nanofluid-based BTMS structures, the performance of mixed Nanofluid (Nf) systems, and the financial and environmental implications of using nanofluids in liquid-based BTMS technologies. According to Can et al. [26], nanofluids represented a promising solution for battery pack thermal management, particularly in terms of improving performance and life cycle outcomes. Their study explored BTMS applications employing the most common soft computing techniques. The use of various machine learning methods in BTMSs has generated valuable evaluation results, which can be used as inputs for future optimisation and performance enhancement efforts. Yang et al. [27] revised a range of cooling strategies – including both active and passive methods – in their BTMS research. Their review covered air cooling, liquid cooling, and PCM-based approaches.

On top of this, the integration of nanofluids with nano-phase change materials (nano-PCMs) to enhance heat dissipation in LIB packs was not thoroughly examined in the open literature. Thus, the current review focuses on nanofluid-based TMSs integrated with PCMs, which improve LIB performance by enhancing thermal control, mitigating thermal runaway, and increasing energy efficiency. This review classifies and quantitatively compares various nanofluids – such as Al_2O_3, CuO, TiO_2, AgO, carbon-based, hybrid, and ternary nanofluids – alongside PCM-enhanced systems, in terms of cooling behaviour, pressure drop performance, and temperature stability. It further investigates nanofluid thermal performance under different microchannel designs, flow rates, and nanoparticle concentrations, besids evaluating the benefits and challenges of hybrid nanofluid–PCM systems. These include issues related to stability, economic feasibility, and scalability. Both experimental and numerical findings are presented to guide future work toward the development of energy-efficient thermal management solutions that optimise next-generation LIB performance.

2. Review methodology

This systematic literature review was conducted to critically examine and synthesise existing academic research on the application of nanofluids and PCMs in the thermal management of LIBs. To ensure the inclusion of high-quality and peer-reviewed studies, the literature search was carried out using three major academic databases: Google Scholar, Scopus, and ScienceDirect. A structured search strategy was employed, using a combination of relevant keywords including ‘thermal management’, ‘nanofluid’, ‘hybrid nanofluid’, ‘lithium-ion batteries’, ‘phase change materials’, ‘PCMs’, and ‘energy efficiency’.

The review focused exclusively on peer-reviewed journal articles published between 2017 and 2025 to capture the most recent developments and emerging trends in this field. Articles were selected based on their contribution to understanding nanofluid-based thermal management designs, experimental and simulation-based analyses, performance evaluations of hybrid systems combining nanofluids and PCMs, and

the overall impact on heat dissipation, thermal regulation, and energy efficiency in lithium-ion batteries (LIBs).

The literature was analysed using a qualitative synthesis method. Specific attention was paid to studies that reported measurable outcomes such as reductions in peak temperature, improvements in thermal conductivity, and enhancements in convective heat transfer. Findings were extracted and compared to identify prevailing trends, recurring limitations, and areas where research is still lacking. Emphasis was also placed on comparative studies between conventional cooling methods and nanofluid-based or hybrid TMSs. Figure 1 illustrates the number of reviewed publications per year, providing a visual representation of the research landscape and growing interest in this field.

3. Enhancing the thermal performance of LIBs with nanofluids and PCMs

Nanofluids, combined with PCMs, are emerging as advanced thermal management techniques for LIBs, aimed at controlling temperature rise and maximising operational efficiency. The use of nanofluids – created by suspending NPs such as Al_2O_3, CuO, and carbon-based materials in base fluids – has led to enhanced heat transfer performance through improved thermal conductivity and convective heat transfer, thereby reducing peak temperatures more effectively than conventional coolants. The integration of PCMs into these systems further improves temperature uniformity and helps delay thermal runaway, as PCMs absorb and store heat via latent heat storage mechanisms. However, the implementation of nanoparticle-based TMSs in EV and energy storage applications requires further optimisation to address challenges such as pressure drops, high costs, and nanoparticle sedimentation.

3.1. Nanofluids in LIBs without PCM

3.1.1. Aluminium nanofluids

To study the electrochemical and thermal behaviour of a commercial 18650 LIB, Sefidan et al. [28] employed a pseudo-2D electrochemical model. A cooling technique was evaluated based on the results of the electro-thermal analysis. The technique comprised immersing the cylindrical LIB cell in a water–Al_2O_3 Nf within a narrow cylindrical tank. Airflow was utilised during the discharge process to eliminate heat from the system. After efficacious testing on a single cell with variable secondary cylinder diameters, the innovative method was extended to the analysis of more severe and thermally hazardous lithium-ion cell configurations. The researchers used 3D transient computational fluid dynamics (CFD) models to inspect how the secondary cylinder can influence the rate of temperature rise. Referring to the outcomes, the novel method efficiently condensed the cells' maximum temperature. As depicted in Figure 2, the maximum temperature drops as the volume fraction rises throughout the simulation. This is ascribed to the growth in thermal conductivity at higher volume fractions.

To upgrade the temperature distribution and cooling capacity of the BTMS throughout both charge and discharge steps, Sarchami et al. [29] achieved a

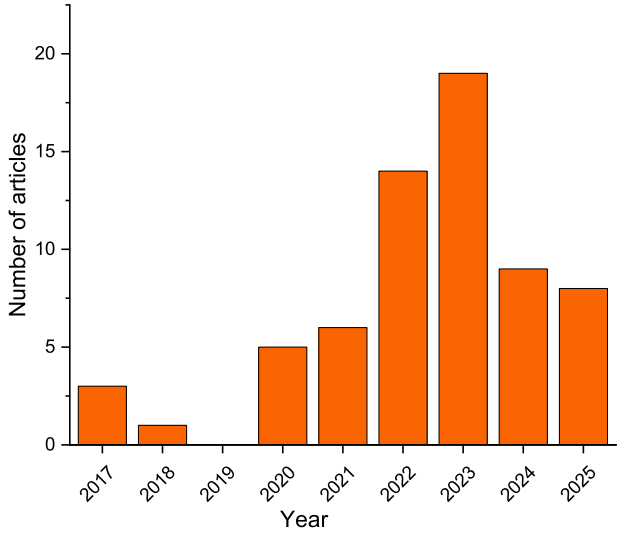

Figure 1. Number of articles and publication year used in this review paper.

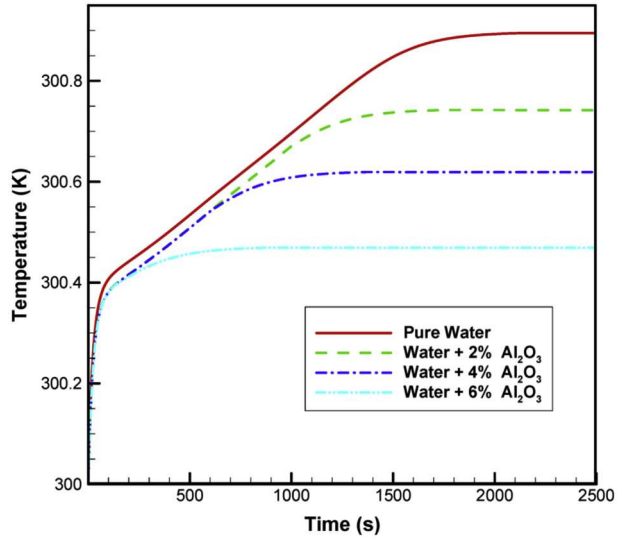

Figure 2. The highest temperature for different volume percentages of NPs [28].

mathematical examination of an innovative liquid cooling system including stair-shaped and wavy channels. These channels used an alumina Nf encased within a copper sheath. The researchers inspected how the thermal efficacy of the battery module can be affected by different parameters, such as inflow velocity, charge/discharge rates, ambient and fluid inlet temperatures, the geometry of the stair channel, the interface areas between neighbouring LIBs, and the contact areas between the LIBs and the wavy channel shell. The simulation outcomes indicated that using a 2 vol.% alumina Nf can reduce the peak temperature and temperature difference during the discharge process by 1.2°C and 0.4°C, respectively, in a comparison to deionised water (DI). Also, an increase in the coolant inflow velocity would decrease both the maximum temperature and the temperature gradient. To simulate various environmental conditions, the battery module was examined across a range of ambient and fluid inlet temperatures. A comparative analysis of the two channel types exposed that the stair-shaped channel can meaningfully minimise the temperature non-uniformity – by 0.19°C during discharge and 0.22°C during charging.

An innovative thermal management tactic for cylindrical LIBs was developed and experimentally established by Sarchami et al. [30]. This system used copper sheaths in combination with liquid cooling channels featuring wavy and stair-shaped geometries. The research examined the impacts of C-rate, alumina nanoparticle concentration, stair channel design, and inflow velocity on cooling performance during charge and discharge cycles. Two volume fractions of alumina NPs, 1% and 2%, were assessed. The outcomes indicated that an increase the concentration of alumina NPs in distilled water expressively mitigated both the maximum temperature and the temperature differential. Also, in increase the inflow velocity not only reduced peak temperatures and temperature non-uniformity but also contributed to a more uniform thermal distribution across the battery module. The stair-shaped channel mitigated the maximum battery pack temperature by approximately 3.59 K and the temperature non-uniformity by 0.65 K during a 5°C discharge process, in a comparison to the straight channel configuration. The results showed that this thermal management technique can reduce the maximum temperature of the battery pack by up to 2.01 K and mitigate the temperature non-uniformity to below 305.13 K under 5°C charge/discharge conditions.

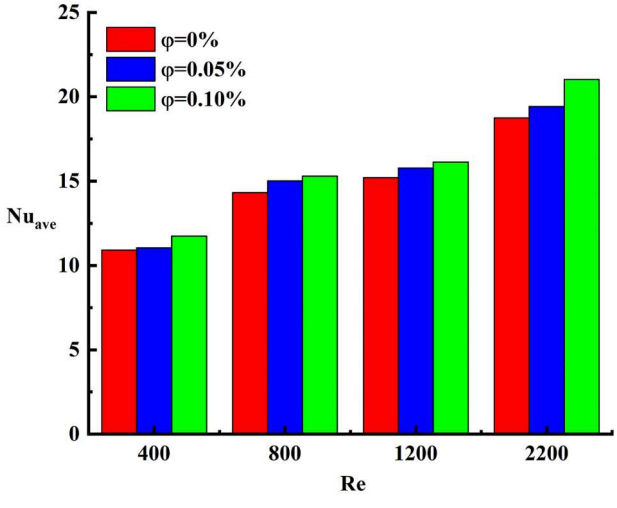

Figure 3. Effect of φ at different Reynolds numbers on heat transfer [32].

Liu et al. [31] developed an experimental system using nanofluids to improve the liquid cooling performance in power batteries. The researchers inspected different Nf concentrations and inlet flow rates to appraise their impacts on cooling competence under various discharge rates and durations. The cooling efficiency of nanofluids was clearly obvious at low discharge rates and flow rates. Nevertheless, a noteworthy drop in cooling efficacy was detected at higher flow rates. Also, no considerable enhancement in cooling performance was noticed at elevated discharge rates and temperatures. High temperatures and flow rates are recognised to degrade nanofluids, with this degradation becoming more noticeable as the Nf concentration rises. Under optimal conditions – explicitly, with 0.9 L/min of flow rate and γ-Al_2O_3/heat transfer fluid Nf concentrations of 0.1%, 1%, and 2% – the battery module's temperature was condensed by 0.24°C, 0.31°C, and 0.52°C, respectively. Consistent developments in cooling performance were documented at 3.77%, 5.02%, and 8.16%.

Another research was conducted by Wang et al. [32] who integrated a parallel microchannel system into a battery pack to lower the temperature of the mounting plate. The study investigated the effects of various parameters, including Reynolds number (Re) and Nf volume fraction, on the battery surface temperature. An increase in Re led to a marked reduction in surface temperature, with numerical results indicating reductions down to 4°C. Increasing the Nf volume fraction to 0.1% enhanced heat transfer by 12.1% and decreased thermal and viscous entropy generation by 5.37% and 23.2%, respectively. However, when Re increased from 400 to 2200, thermal and viscous entropy generation rose sharply, by 253.71% and 389.80%, respectively. Following extensive optimisation, the researchers identified channel 39 as optimal,

achieving a 24% increase in pressure ratio and a 17% improvement in the Nusselt number. An increase in the Nf volume fraction was consistently associated with improved heat transfer performance of the battery pack plate. As illustrated in Figure 3, when Re increased from 400 to 800, the heat transfer quantity rose to 10.91 and 14.32, respectively.

In 2023, Anqi [33] investigated the impact of a serpentine microchannel on the surface temperature of a battery. Numerical methods were employed to model the thermal behaviour and Nf flow within the serpentine microchannel and across the battery surface. The research demonstrated that the use of nanofluids could enhance heat transfer from the serpentine microchannel to the battery by up to 20%. Among the examined parameters, the Re emerged as the most influential factor in improving heat transfer. Within a Re range of 25–150, heat transfer increased by approximately 6.34–12.75%. Furthermore, compared to conventional channel walls, hydrophobic microchannel walls improved heat transfer efficiency by 14%. The significance of the Nf volume fraction in enhancing battery cooling is illustrated in Figure 4. The data show that heat transfer between the battery surface and the serpentine micro-channel is directly proportional to the Nf volume fraction.

By integrating phase change cooling, Nf cooling, and thermal insulation materials, Ouyang et al. [34] developed a BTMS that is both efficient and energy-saving. Initially, the electrochemical, thermal, and fluid models were combined to construct the system model, which was subsequently validated. The system was then evaluated under two different operational scenarios. Under harsh conditions, Scheme 6 reduced the maximum battery temperature from 980.5 K to 380.3 K, and heat was effectively dissipated over time. Additionally, an improved version of the scheme further reduced the economic index by 22% and the maximum battery temperature by 23% compared to Scheme 6. While the absolute maximum temperature varies across different Nf volume fractions, Figure 5 illustrates that the overall temperature trend of the battery remains consistent. The highest recorded temperature was 405.24 K when the volume fraction was 0%, i.e. when pure water was used as the coolant. In contrast, when the Nf volume fraction was increased to 3%, the maximum temperature decreased to 400.70 K.

Jha et al. [35] proposed an innovative design for a curved inverted-L grooved channel cold plate to enhance the thermal management of LIB packs. This design utilised an antifreeze-based alumina Nf to achieve efficient cooling. The researchers systematically evaluated the thermal performance of the proposed system by varying parameters such as channel width, number of channels, and coolant type. They compared its effectiveness with both a reference module and a serpentine channel configuration within a mini-channel cooling plate. Battery behaviour was simulated using an analogous circuit model. The optimal thermal performance was achieved using five 6 mm wide channels etched into an aluminum cold plate, with a coolant composed of 1% Al_2O_3 in a 20:80 ethylene glycol–water nanofluid. The optimised system was then tested using a 1P6S battery pack under both static (constant 5C-rate) and dynamic (aggressive drive cycle) load conditions. Under the 5C-rate discharge scenario, the proposed cooling system successfully reduced the battery

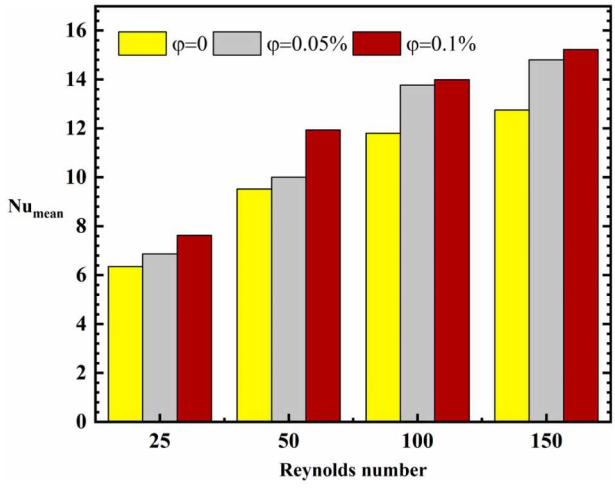

Figure 4. Heat transfer effects of φ at different Reynolds number levels [33].

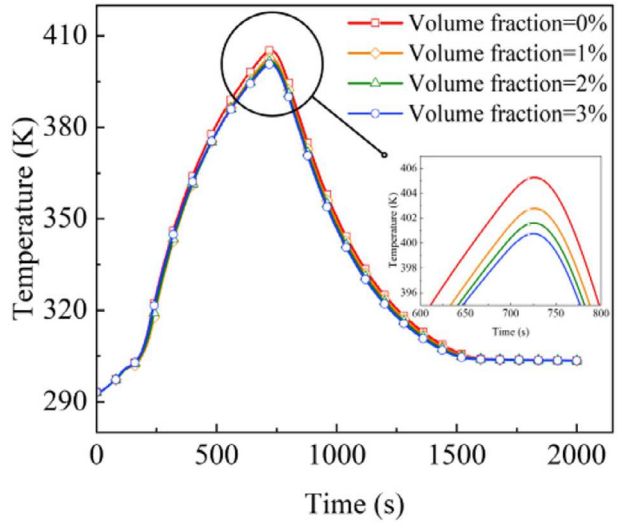

Figure 5. Impact of the volume fraction of NPs on the new BTMS: (a) temperature variation under various nanoparticle volume fractions [34].

pack's maximum temperature from 341.4 K to 300.7 K by the end of discharge.

Banerjee and Nidhul [36] investigated a novel immersion cooling configuration featuring V-shaped fins and dielectric fluids – specifically deionised water, Novec 7200, and n-heptane – as coolants. A two-phase mixture model was employed, and the system was evaluated under high discharge rates of 3C and 5C, maintaining constant coolant volume and mass flow rate. NPs were uniformly dispersed throughout the system. The V-shaped fins enhanced fluid mixing through secondary flow, significantly reducing the maximum cell temperature and improving temperature uniformity across the battery pack. At a discharge rate of 3C, deionised water Nf achieved a temperature reduction of 5 K. At 5C, even in the absence of fins, a 9 K reduction was observed. Among the tested coolants, Novec 7200 provided the best temperature uniformity, maintaining a maximum temperature variation of less than 0.5 K even at a 5C discharge rate. When compared with deionised water, Novec 7200 achieved superior thermal homogeneity and the lowest overall temperature rise. Furthermore, the power required to pump the Nf was negligible compared to the power output of the battery pack, highlighting the system's energy efficiency.

Referring to the aforementioned researches of aluminium nanofluids, it can be said that the use of aluminum nanofluids have demonstrtaed significant enhancement in thermal management for LIBs. Immersing LIBs in water-Al_2O_3 NFs has deduced clear reductions in peak temperatures during discharge. Inventive cooling channel designs have improved temperature distribution and cooling capacity, attaining lower peak temperatures in a comparison to conventional approaches. Optimal concentrations and flow rates of NFs can aid to maximise cooling efficacy. Microchannel systems and serpentine designs can meaningfully enhanced heat transfer, while combined phase change cooling with NFs has verified active for thermal management. Also, immersion cooling configurations featuring V-shaped fins attained remarkable temperature uniformity and reductions under high discharge rates. Accordingly, the above results can signify the potential of aluminum nanofluids in improving battery thermal management systems.

3.1.2. Aluminium nanofluids Cu-nanofluids

In their research, Wu and Rao [37] employed a lattice Boltzmann (LB) model to simulate natural convection in a Cu-water nanofluid-based battery thermal management (BTM) system. The researchers authorised their numerical model by resolving the case of a hollow cylinder with a uniformly distributed heat source to assure its accurateness. The research was achieved for Nf volume fractions rang from 0% to 6%, with Rayleigh numbers spanning from 10^3 to 10^6. The outcomes established that the inclusion of copper NPs enhanced both the temperature uniformity and the cooling performance of the BTM system. Precisely, using a 6% Cu-water Nf at a Rayleigh number of 3×10^3 can reduce the maximum temperature by about 6.5%. Also, the intensity of heat transfer was meaningfully enriched due to stronger natural convection, as the Rayleigh number rises from 10^4 to 10^6.

Zhao et al. [38] primarily concentrated on the subject of heat generation in lithium-ion battery packs (LIBPs). They inspected the influence of cooling performance on the temperatures of three LIBPs arranged in series within a duct. The thermal conductivity of the working fluid was improved by the inclusion of copper oxide (CuO) NPs to pure water. The outcomes elaborated that at a Re number of 60, increasing the volume fraction of NPs from 0% to 4% can mitigate the maximum temperatures of LIBP 1, 2, and 3 by 2.19°C, 2.26°C, and 2.64°C, respectively. However, at higher Re numbers, the addition of NPs had little to no significant effect on the maximum temperatures of the LIBPs. As shown in Figure 6, the nanoparticle concentration had minimal impact on the performance efficiency (η_p) at $Re = 80$ and $Re = 100$. Additionally, Figure 7 illustrates that at $Re = 60$, increasing the nanoparticle volume fraction from 0% to 4% resulted in a 41% rise in pressure drop, indicating a trade-off between thermal enhancement and hydraulic performance.

Using four $LiFePO_4$batteries, Qawasmeh et al. [39] proposed a novel method for evaluating TMSs for LIBPs. The researchers tested several advanced configurations, including a semi-passive system employing forced water cooling and a passive system incorporating a PCM enhanced with expanded graphite. Leveraging the improved thermal properties of NPs, a key innovation involved replacing water with a Nf within a single cold plate surrounded by a PCM composite. To further optimise cooling performance, enhanced cold plate designs and two-dimensional flow dynamics were implemented in both a three-plate system and a more complex-plate system. Among all configurations, the complex-plate system with Nf demonstrated the most effective performance – reducing the maximum temperature from 88.17°C in the passive system to 73.03°C and extending the operating temperature threshold by 7.41%. The impact of NPs on thermal performance was evident, as they contributed to a 9.46% reduction in temperature. Notably, the complex-plate system outperformed the three-plate configuration in terms of efficiency, achieving

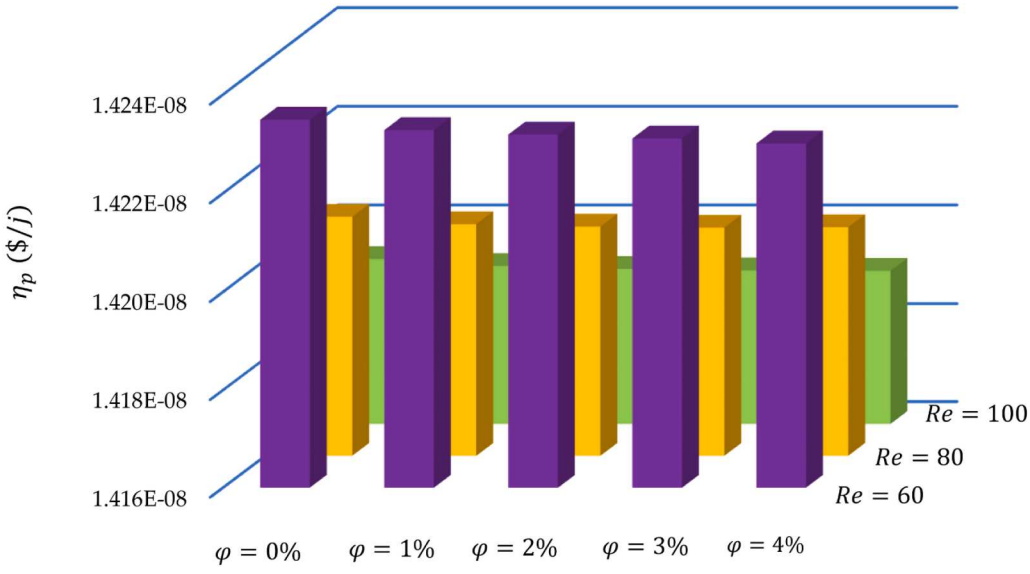

Figure 6. The value of performance efficiency for different Reynolds numbers and volume fractions [38].

superior cooling with lower pumping power requirements.

To summarise the above research of aluminium nanofluids Cu-nanofluids, the use of aluminum and copper nanofluids (NFs) has significantly enhance the battery thermal management systems. Statistically, temperature uniformity and cooling performance were improved via using copper-water NFs (6% volume fraction) by mitigating peak temperatures by 6.5%. Also, the inclusion of copper oxide NPs to pure water can result in temperature reductions of more than to 2.64° C in lithium-ion battery packs, despite higher Reynolds numbers would diminish their influence. An innovative practice for thermal management systems showed that a complex-plate configuration with NFs can meaningfully reduce maximum temperatures from 88.17°C to 73.03°C, besides upgrading cooling efficacy and prolonging operating temperature thresholds.

3.1.3. Cu-nanofluids TiO_2-nanofluids

For EV LIBs, Chen and Li [40] evaluated a pulsing heat pipe (PHP) system using a titanium dioxide (TiO_2)-based Nf under variable environmental and operational conditions. At an ambient temperature of 35°C and a discharge rate of 1C, the battery's maximum temperature remained below 42.22°C, and the temperature gradient across the battery did not exceed 2°C. The system achieved an active thermal enhancement rate of up to

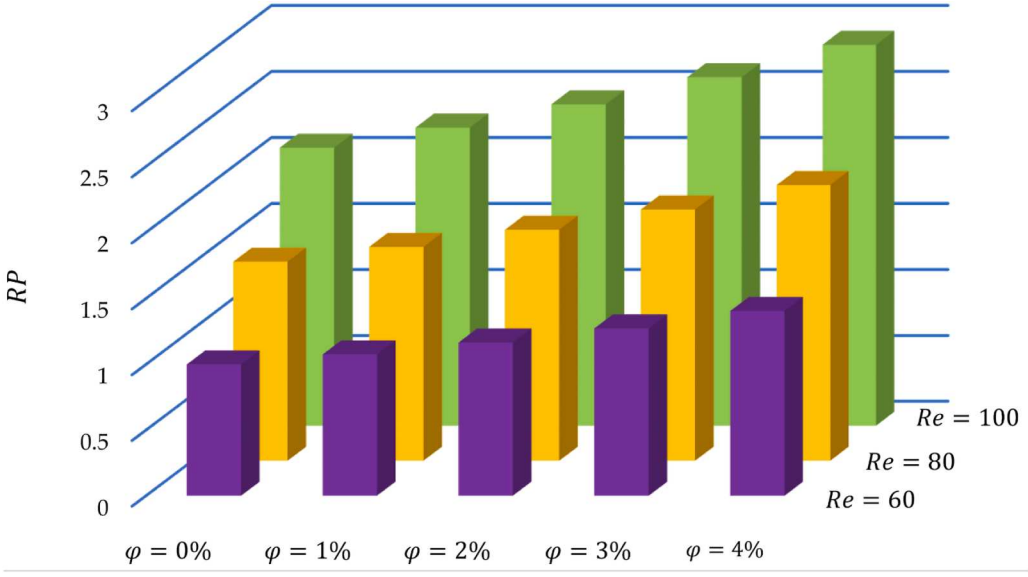

Figure 7. The pressure ratio between each instance and the reference case under the circumstances Re = 60,φ = 0% [38].

60%, along with a more uniform temperature distribution across the battery surface. The LIBs also exhibited favourable thermal performance in terms of surface temperature gradient, temperature rise, and maximum temperature at the end of discharge under 0.5C, 1C, and 1.5C rates. The results demonstrated that the PHP-based TMS utilising a TiO_2 Nf offered excellent heat dissipation capabilities, effectively reducing temperature gradients and enhancing thermal uniformity across the battery surface. Accordingly, the TiO_2-PHP system guaranteed that the LIB operated powerfully within a temperature range of 20°C to 50°C.

Wiriyasart et al. [41] conducted a computational analysis of Nf flow through a corrugated mini-channel in an EV battery cooling module, focusing on temperature distribution and pressure drop. The EV battery module consisted of 444 cylindrical 18650-type LIB cells. Among the investigated parameters, coolant flow direction, mass flow rate, and coolant type were found to have the greatest influence on temperature distribution. As shown in Figure 8, the proposed cooling module (Model II) using nanofluids achieved a maximum temperature reduction of 28.65% compared to the conventional cooling module (Model I). However, as illustrated in Figure 9, this improvement came with an associated increase in pressure drop. Nevertheless, nanofluids outperformed water-based coolants by providing greater overall cooling capacity.

Saghir et al. [42] explored methods to improve the cooling mechanisms of LIBs. Two primary cooling fluids were tested: deionised water and TiO_2-based nanofluids with volume concentrations of 0.1%, 0.5%, and 2%, each diluted in deionised water. The cooling system employed six rectangular channels, with heights ranging from 2 mm to 4 mm. Designed for commercial applications, the system sandwiches two sets of LIBs between channels made from various materials. The results indicated that metallic NPs (i.e. nanofluids) enhanced the thermal performance of water as a cooling medium. Although the use of nanofluids led to an increase in pressure drop, heat transfer was improved by approximately 12%. All three Nf formulations, along with pure deionised water, were evaluated based on performance metrics illustrated in Figure 10. A distinct nonlinear relationship was observed between the inlet velocity and cooling performance. At higher flow rates, the high-concentration titanium dioxide Nf (1 vol.% TiO_2 / 99 vol.% water) delivered superior thermal performance. Figure 11 compares surface temperatures for a 1C-rate battery cooled with nanofluids (without pin fins) and a 1C-rate battery cooled with water (with pin fins).

Saghir and Bicer [43] compared the thermohydraulic performance of a straight channel with that of a wavy channel configuration, using water as the cooling fluid. The results showed that the wavy channel outperformed the straight channel in terms of performance assessment criteria, albeit at the cost of increased pressure loss. Among the various fluids tested – including water, isopropanol, a binary mixture of ammonia and water, and a TiO_2-based nanofluid – ammonia was identified as the most effective cooling fluid. The average Nusselt number for batteries operating at a 1C-rate is illustrated in Figure 12. Figure 12 clearly indicates a noticeable increase in heat transfer with higher nanoparticle concentrations. As shown in Figure 13, the performance assessment criteria take into account both thermal and hydraulic effects. The results suggest minimal differences in performance between Nf concentrations of 0.1 and 1 vol.%, indicating diminishing returns at higher concentrations.

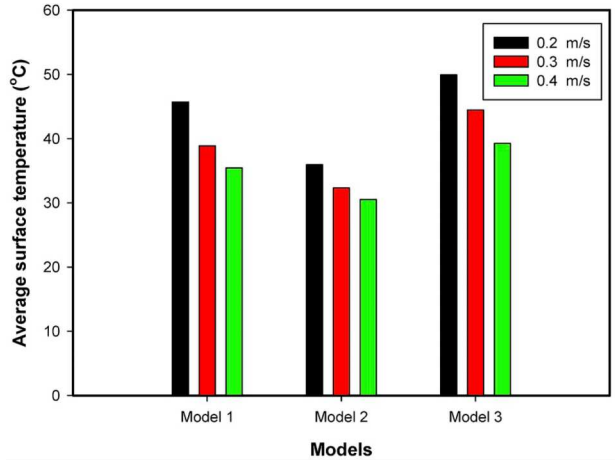

Figure 8. Coolant velocity's impact on output temperature [41].

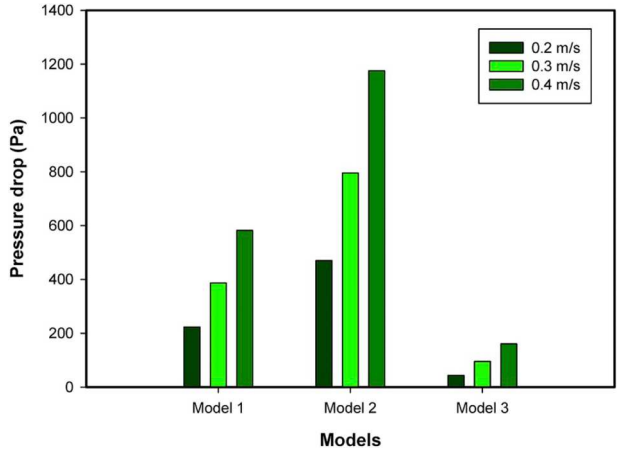

Figure 9. Coolant pressure drop variation measured from several cooling modules [41].

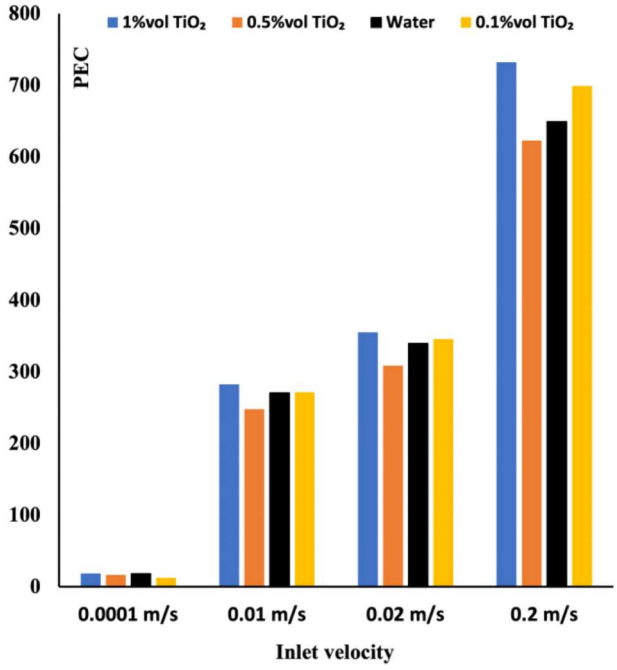

Figure 10. PEC for batteries that are 1C (Hc = 2 mm) [42].

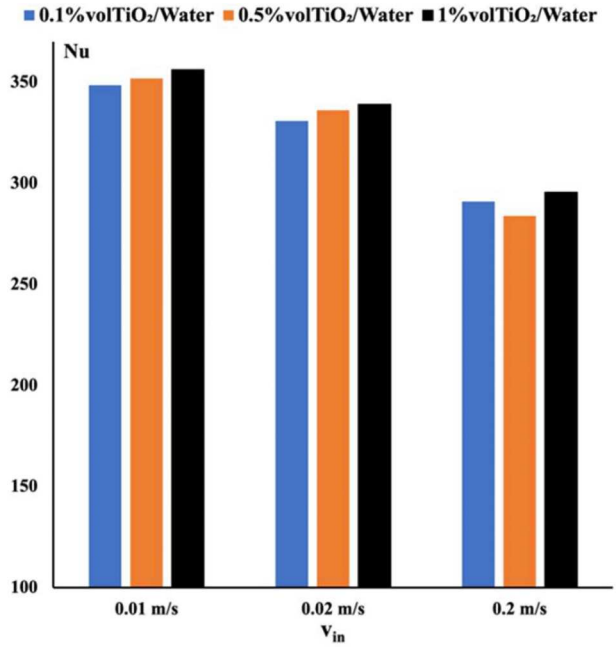

Figure 12. Variation in the Nusselt number with varying concentrations of TiO_2 [43].

The above revised studies can elucidate the effectiveness of copper and titanium dioxide nanofluids to remarkably enhance battery thermal management systems for electric vehicle LIBs. First of all, using TiO_2-based NFs in a pulsing heat pipe system can efficiently maintain battery temperatures below 42.22°C, attaining a temperature gradient of under 2°C and a thermal improvement rate of up to 60%. Also, a corrugated mini-channel cooling module utilising NFs can achieve a maximum temperature reduction of 28.65% in a comparison to conventional approaches, even though it incurs a higher pressure drop. TiO_2 NFs introduced a heat transfer improvement by around 12%, with high-concentration formulations bringing greater thermal performance at elevated flow rates.

3.1.4. Carbon-nanofluids

Yang et al. [44] developed a hybrid cooling system for LIBs that utilised nanofluids and expanded surfaces

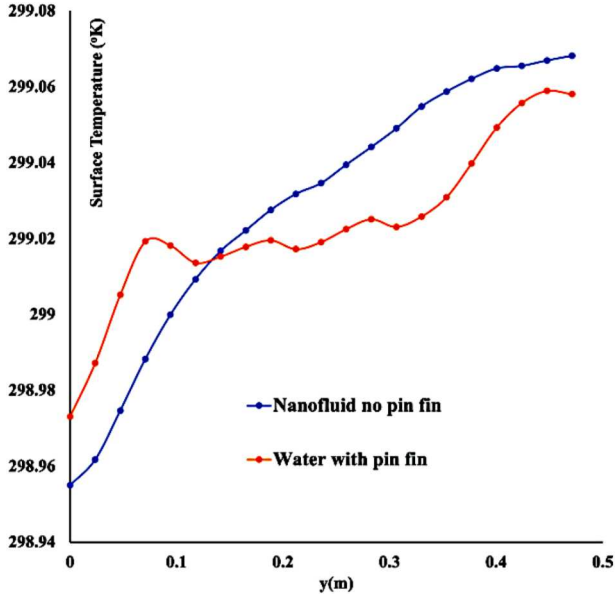

Figure 11. Temperature at the top of the battery cell. (Inlet speed = 0.2 m/s) [42].

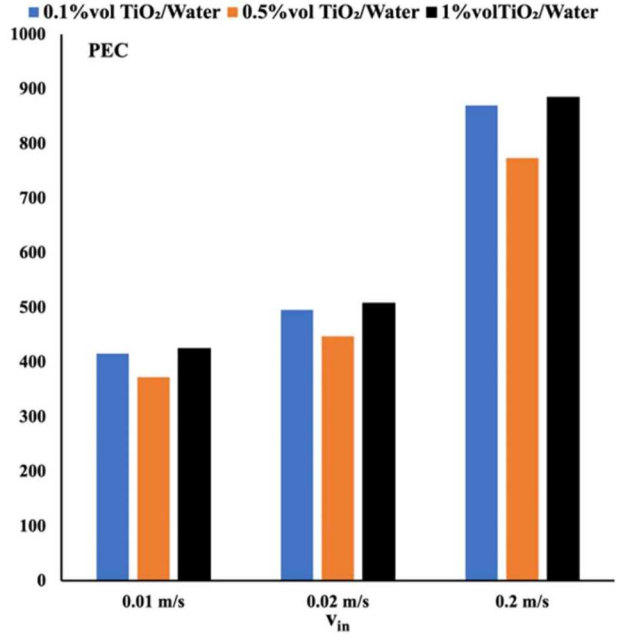

Figure 13. Variation in PEC with varying concentrations of TiO_2 [43].

(microchannels) to maintain effective thermal regulation. During charging, a solar-powered system monitored the battery's performance. Within the cooling setup, a non-Newtonian hybrid Nf containing carbon nanotubes was circulated. The system was simulated numerically using the Galerkin finite element method (FEM) to analyse the flow behaviour and heat transfer features of the non-Newtonian Nf around the battery. The outcomes stated that utilising the A-3 configuration at a Re = 100 can reduce the maximum battery cell temperature by 0.4°C in a comparison to the conventional model,. Moreover, among all tested models, model A-2 attained the lowermost maximum temperature at a Re = 1000, 0.11°C lesser than the traditional model. Across all the tested configurations, the utilise of hybrid NPs can lower the initial temperature and increase the pressure drop at any Re number. Finally, this research verified that the inclusion of carbon nanotubes to the base fluid can enhance battery performance and thermal efficiency, combined with the use of nanofluids in microchannel systems.

Aberoumand et al. [45] examined a Nf based on electrochemical graphene oxide (EGO) in a vanadium (IV) electrolyte, specifically observing its rheological behaviour, thermal conductivity, and electrical conductivity under different weight concentrations and bulk temperatures. The Nf displayed optimum viscosity, electrical and thermal conductivities, and colloidal stability at a weight concentration of 0.05 wt.%. The research determined that the flow battery's performance can be enhanced in terms of electrochemical activity at the electrode surface and overall thermal management. The perfections were ascribed to improvements of up to 12% in electrical conductivity and 4% in thermal conductivity. Rheological testing also exposed that at weight concentrations above 0.05 wt.%, the Nf began to display non-Newtonian behaviour, transitioning from its initial Newtonian characteristics.

A hybrid oscillating heat pipe (OHP) was developed by Zhou et al. [46] to efficiently dissipate heat from EV batteries during rapid charging and discharging cycles. The OHP comprises of a copper flat-plate evaporator with parallel circular channels and a capillary copper-tube condenser. carbon nanotube (CNT) nanofluids and ethanol–water mixtures were selected as working fluids, each with a volumetric filling ratio of 35%. The ethanol–water mixture had a 1:1 volume ratio and was infused with CNTs at mass concentrations ranging between 0.05 wt.% to 0.5 wt.%. The experimental outcomes showed that a vertically oriented OHP charged with CNT nanofluids can offer superior performance in terms of start-up behaviour and heat transfer efficiency in a comparison to the ethanol–water solution. The average evaporator temperature was decreased to 43.1°C, at a CNT concentration of 0.2 wt.%, while the thermal resistance decreased to 0.066°C/W at a power input of 56 W – demonstrating drops of 9.8°C and 0.278°C/W, respectively, in a comparison to the ethanol–water mixture.

Kim and Park [47] experimentally inspected the consequence of carbon-based NPs added to the electrolytes of vanadium redox flow batteries on their electrochemical performance. A number of techniques including Raman spectroscopy, X-ray diffraction (XRD), and X-ray photoelectron spectroscopy (XPS) exposed that the NPs, which serve as electrochemical reaction sites, possess structural defects. Cyclic voltammetry outcomes indicated that nanofluidic electrolytes can exhibit enhanced redox kinetics and mass transport in a comparison to pure electrolytes. Specifically, VO^{2+}/VO_2^+ electrolyte ions demonstrated mass transfer improvements of 17.2% and 59.8% during oxidation and reduction processes, respectively, while V^{2+}/V^{3+} ions exhibited mass transfer rates that were 5.6 and 1.2 times higher than those of VO_2^+/VO_2^+ electrolytes, respectively. Overall, the use of nanofluidic electrolytes enhanced electron and mass exchange at the active interface area. According to the redox mechanism, VO^{2+}/VO_2^+ electrolytes provide a larger active area, while V^{2+}/V^{3+} electrolytes significantly reduce the activation energy required for redox reactions. These enhanced mass transport properties make nanofluidic electrolytes particularly well-suited for minimising concentration polarisation losses.

Aberoumand et al. [48] experimentally investigated the long-term impact of using reduced graphene oxide (rGO) nanofluidic electrolytes on the performance of vanadium redox flow batteries. The active surface area of the electrodes was found to be approximately 130% and 135% higher for the positive and negative electrode samples, respectively, when exposed to a 1.0 wt.% Nf compared to electrodes in contact with pure electrolyte. The charge and discharge performance of the flow battery improved significantly when using the optimised nanoparticle concentration of 0.1 wt.%, particularly across a range of current densities. At this optimal concentration, energy efficiency and voltage efficiency were enhanced by 15% to 24% and 8% to approximately 21%, respectively, at current densities ranging from 25 to 150 mA cm^{-2}. Electrolytes containing 0.1 wt.% Nf also exhibited reduced ohmic resistance and polarisation effects.

Mitra et al. [49] developed an innovative TMS for cylindrical 18650 LIB cells, evaluating its cooling performance under various discharge rates. The system employed indirect liquid cooling using single and dual aluminum serpentine tubes. The researchers assessed

nanofluids prepared with ethylene glycol and water at three different volume fractions (0.15%, 0.3%, and 0.45%), as well as comparisons with pure water and binary mixtures. At 0.45% multi-walled carbon nanotubes (MWCNTs), the single-channel, dual-channel with counter-flow, and dual-channel with parallel flow configurations achieved maximum average temperature reductions of 6.9°C, 11°C, and 10.2°C, respectively, at a 2.1C discharge rate. The most effective cooling was observed in the dual-channel counter-flow configuration, achieving temperature reductions in the range of 8.6–13°C depending on the working fluid. This configuration also maintained excellent thermal uniformity, with a maximum temperature variance of only 1.5–3°C – well within the safe operating limits for avoiding thermal runaway. With 0.45% MWCNTs, the pressure drop increased by 13% compared to water in the single-channel setup and by 14% in the dual-channel configuration.

Rana et al. [50] achieved an experimental assessment of a developed liquid-based BTMS for LIBs under variable discharge rates (C-rates). The researchers evaluated the impacts of a number of parameters – including working fluid type, C-rates, number of cooling channels, and flow configurations – on the system's thermal performance. The comparison comprised pure water, a binary fluid mixture (70% water + 30% ethylene glycol), and MWCNT-based nanofluids at volume fractions (φ_v) of 0.15%, 0.3%, and 0.45% in the binary fluid. The results indciated that nanofluids reliably outpaced both water and the binary fluid in terms of cooling efficacy at 0.5C, 1.2C, and 2.1C discharge rates. Cooling performance improved with increases in nanoparticle concentration, the number of channels, and optimised flow configurations. In configurations I, II, and III, the maximum temperature reductions achieved using nanofluids with 0.45% φ_v MWCNTs were 8.7°C, 11.8°C, and 17.1°C, respectively.

As discussed above, one can reveal that carbon nanofluids can significantly make an advancement in thermal management systems for LIBs. A hybrid cooling system uses carbon nanotube nanofluids and microchannels can reduce the maximum battery cell temperatures by more than 0.4°C in a comparison to conventional approaches. The optimal concentrations of electrochemical graphene oxide (EGO) nanofluids also indicated an improvement in electrical and thermal conductivities of more than 12%. Furthermore, a superior heat transfer performance was assured using a hybrid oscillating heat pipe using CNT nanofluids, which enables to significantly lower evaporator temperatures in a comparison to ethanol-water mixtures. The integration of carbon-based nanofluids in vanadium redox flow batteries can improve the mass transport and electrochemical kinetics, which causes reduced polarisation losses and improvement in energy efficiency. Also, innovative cooling systems with multi-walled carbon nanotubes elaborated maximum temperature reductions of 17.1°C at higher discharge rates.

3.1.5. Silver-nanofluids

A new BTMS for 18650- and 21700-type LIBs was developed by Tousi et al. [51] using a silver oxide (AgO) nanofluid. The goal of the system was to maintain temperature uniformity and keep the maximum temperature of the battery pack within the optimal operating range. The researchers achieved numerical simulations to analyse the impact of discharge rate, Nf volume fraction, and coolant inflow velocity on the thermal performance of the battery pack at high discharge rates (3C, 5C, and 7C). A complete contrast between the 18650 and 21700 battery packs was achieved. The outcomes indicated that an increase in both inflow velocity and Nf volume fraction can meaningfully mitigate the battery pack's maximum temperature and temperature differential. Precisely, with optimal inflow velocity and Nf concentration, the maximum temperature and temperature differential were preserved below 305.59 K and 1.07 K, respectively, while utilising a 7C discharge rate.

Jahanbakhshi et al. [52] explored the advantages of using a biologically synthesised silver–water/ethylene glycol Nf as a working fluid for thermal management. The researchers inspected how parameters such as nanoparticle volume fraction (φ), Re number, and the configuration of fluid inlets and outlets impacted the thermal performance and surface temperature distribution of the battery. In all cases, the outcomes showed that heat sinks can efficiently reduce the battery surface temperature. The inclusion of the Nf aided to preserve temperatures within a safe operating range. The battery surface temperature was reliably preserved between 300 K and 310 K, along with improved thermal uniformity, while using counterflow configurations in microchannels and microtubes. However, battery temperatures ranged from 303 K to 312 K, and the temperature difference across the surface never exceeded 5°C while using the parallel flow. Furthermore, increases in both Re and φ led to higher entropy generation within the system.

Azizi et al. [53] conducted an experimental assessment of the thermo-hydraulic properties of silver–water nanofluids at concentrations of 0.1, 0.45, and 0.8 wt.% flowing through a cylindrical microchannel heat sink in the laminar flow regime. All tests were

performed under a constant heat flux of 56.8 kW/m^2, with Reynolds numbers ranging from 400 to 1300. The most efficient scenario was observed for the 0.8 wt.% Nf at Re = 850, which achieved a thermal performance factor (TPF) of approximately 1.35 and demonstrated a 67.1% enhancement in the Nusselt number compared to the base fluid. Under this optimal condition, the pressure loss remained below 0.2 bar due to the properties of the silver nanofluid. To optimise performance outcomes, Design-Expert statistical software was utilised based on response surface methodology (RSM). The results clearly indicated that Reynolds number had a stronger positive influence on the local heat transfer coefficient than nanoparticle concentration.

Rahmani et al. [54] investigated the feasibility of implementing topological modifications to improve the TMS of battery packs. These modifications were found to be both technically and economically viable. A 3 vol.% AgO–water Nf was also tested for its effects on system performance. The researchers focused on a nanofluid-cooled pack of ten cylindrical batteries subjected to constant heat flux. They also evaluated the effects of repositioning the inlet and outlet ports and adding one or two guiding plates to control the flow direction. Simulations were conducted for Reynolds numbers ranging from 1000 to 2000, as determined by the inlet diameter of the battery pack. As the Re number increased from 1000 to 2000, the Nusselt number improved by up to 30%. Topological adjustments alone were found to increase the Nusselt number by more than 25%, while maintaining a pressure drop increase of no more than 50%. Compared to a basic cooling system without guiding plates, the optimised configurations achieved a temperature distribution that was approximately 50% more uniform.

In a complementary study, Rahmani et al. [54] analysed the enhancement of BTMS through low-cost, easily implementable topological changes. The same 3 vol.% AgO–water Nf was employed, and the researchers again focused on a pack of ten cylindrical batteries under constant heat flux. Figure 14 presents the results of varying the inlet/outlet port positions and introducing one or two guiding plates to manage fluid flow. The analysis, conducted for Reynolds numbers ranging from 1000 to 2000, reaffirmed that increases in Re improved thermal performance, with the Nusselt number rising by up to 30% and topological enhancements contributing more than 25% of that improvement. The associated pressure drop remained below the 50% threshold. In comparison to the baseline system without guiding plates, the redesigned configurations achieved significantly more uniform temperature distributions – up to 50% improvement. Figure 15 illustrates the temperature distributions for all scenarios at Re = 2000 with Nf cooling. For Case 1, a high-temperature zone was clearly observed near the bottom of the pack at the inlet region.

Using a mesh plate and an AgO-based nanofluid, Sarchami et al. [55] developed a novel TMS designed to control the maximum temperature and maintain thermal uniformity during the rapid discharge of a 21700-type LIB pack. Numerical simulations were conducted to evaluate the thermal performance at a 7C discharge rate, considering various parameters such as coolant inflow velocity, AgO nanoparticle volume fraction, mesh plate geometry, inlet/outlet hydraulic diameters, and flow direction. The results showed that increasing both the inflow velocity and the Nf volume fraction significantly reduced the maximum temperature and the temperature differential. Compared to deionised (DI) water, the use of a 4% volume fraction AgO-based Nf resulted in a 3.08% reduction in maximum temperature and a 60.7% reduction in temperature differential. Specifically, increasing the inflow velocity led to a further reduction of 0.64 K in maximum temperature and 0.3 K in temperature differential. Additionally, variations in the inlet and outlet hydraulic diameters and flow directions had a substantial impact on both the maximum and temperature uniformity across the battery pack.

Based on the critical analysis of the aforementioned studies of silver-based nanofluids, a notable improvement in thermal management systems for LIBs was deduced. An innovative thermal management system uses silver oxide (AgO) nanofluids can successfully preserved temperature uniformity, holding a maximum temperature below 305.59 K at high discharge rates (7C) with optimal coolant inflow and nanofluid concentrations. Also, an efficient battery with maintained surface temperatures within a safe range was assured for biologically synthesised silver-water/ethylene glycol nanofluids particularly with counterflow configurations. Silver-water nanofluids indicated an enhancement in thermal performance factors, while attaining a 67.1% increase in Nusselt number at optimal concentrations. Finally, AgO nanofluids presented a reduction in maximum temperature and temperature differentials during rapid discharge, overtaking deionised water.

3.1.6. Fe-nanofluids

Yetik and Karakoc [56] employed nanofluids – mixtures of NPs and refrigerants in varying proportions – to cool battery systems. The Nf combinations included engine oil (EO + 3% Fe_2O_3, EO + 4% Fe_2O_3, EO + 6%

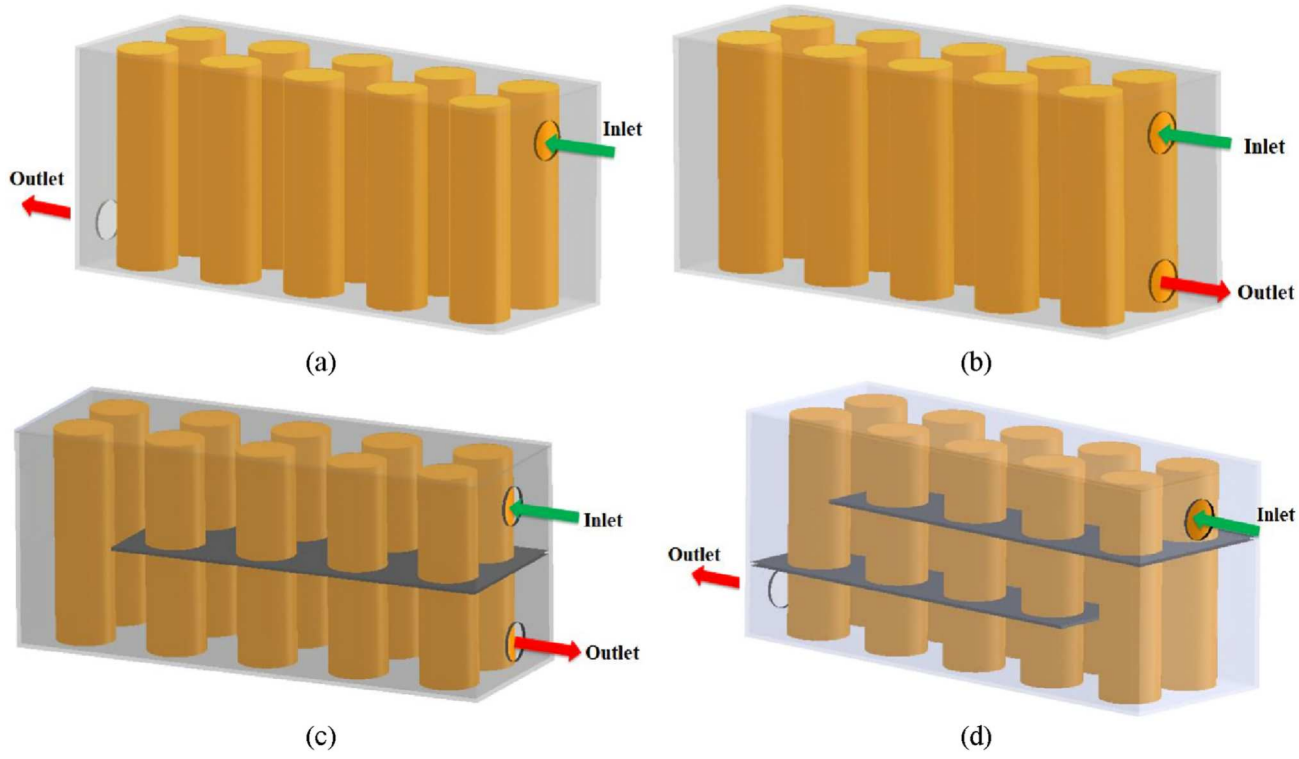

Figure 14. Various examed geometries (a) instance 1, (b) case 2, (c) case 3, and (d) case 4, the [54].

Fe_2O_3) and water-based mixtures (H_2O + 3% Fe_2O_3, H_2O + 4% Fe_2O_3, H_2O + 6% Fe_2O_3). Each battery within the module was individually tested for temperature. The study analyzed the thermal and electrical properties of the battery model under different inlet velocities, discharge rates, and Nf volume fractions. The results showed that increasing the Fe_2O_3 concentration from 3% to 6% caused a temperature change of only 0.05 K when water was used as the refrigerant, while a more substantial change of 1.15 K was observed when EO was used. Overall, the water-based nanofluids outperformed the EO-based counterparts. When analysing the effect of inlet velocity, the minimum temperature change for H_2O + 6% Fe_2O_3 was 0.2 K, and the maximum temperature difference reached 1 K.

Dilbaz et al. [57] investigated a TMS for a 20 Ah rectangular battery pack using two cooling fluids: pure water and a hybrid Nf composed of nanodiamond (ND)–Fe_3O_4 particles in a water–ethylene glycol (W/EG) mixture. The system was tested with Re numbers ranging between 100 to 800 and fin counts from 5 to 25. Discharge rates of 3C, 4C, and 5C were evaluated with nanoparticle volume fractions between 0% and 2%. The findings showed that increasing both the Re number and nanoparticle volume fraction improved the battery pack's thermal performance. Specifically, using a 2 vol.% ND–Fe_3O_4+ W/EG hybrid Nf at Re = 800 reduced the temperature differential by 70.35% and the maximum temperature by 23.1%, compared to water at the same Re number. Performance was further enhanced by increasing the number of fins: the 25-fin model exhibited a 13.8% lower temperature differential than the 5-fin configuration.

Yetik et al. [58] used the NTGK model to conduct thermal and electrical analyses of the battery system. They investigated the effects of various control parameters – including nanoparticle mixing ratio, inlet velocity, ambient temperature, and C-rate – on thermal management performance. A Taguchi L16 orthogonal array was used to systematically evaluate these factors. The results indicated that the battery's temperature increased with rising C-rate and decreased with higher nanoparticle mixing ratios. Among all variables, the C-rate had the greatest influence on maximum battery temperature and temperature uniformity, while the mixing ratio had the least impact. The lowest maximum battery temperature (294 K) was achieved under the following conditions: inlet velocity of 0.04 m/s, mixing ratio of 5, C-rate of 2, and ambient temperature of 283 K. To achieve optimal temperature uniformity, the best parameters were a mixing ratio of 3, inlet velocity of 0.04 m/s, C-rate of 2, and ambient temperature of 313 K. These findings emphasise the importance of carefully monitoring the C-rate during discharge, as it has a far greater effect on thermal performance than the nanoparticle mixing ratio.

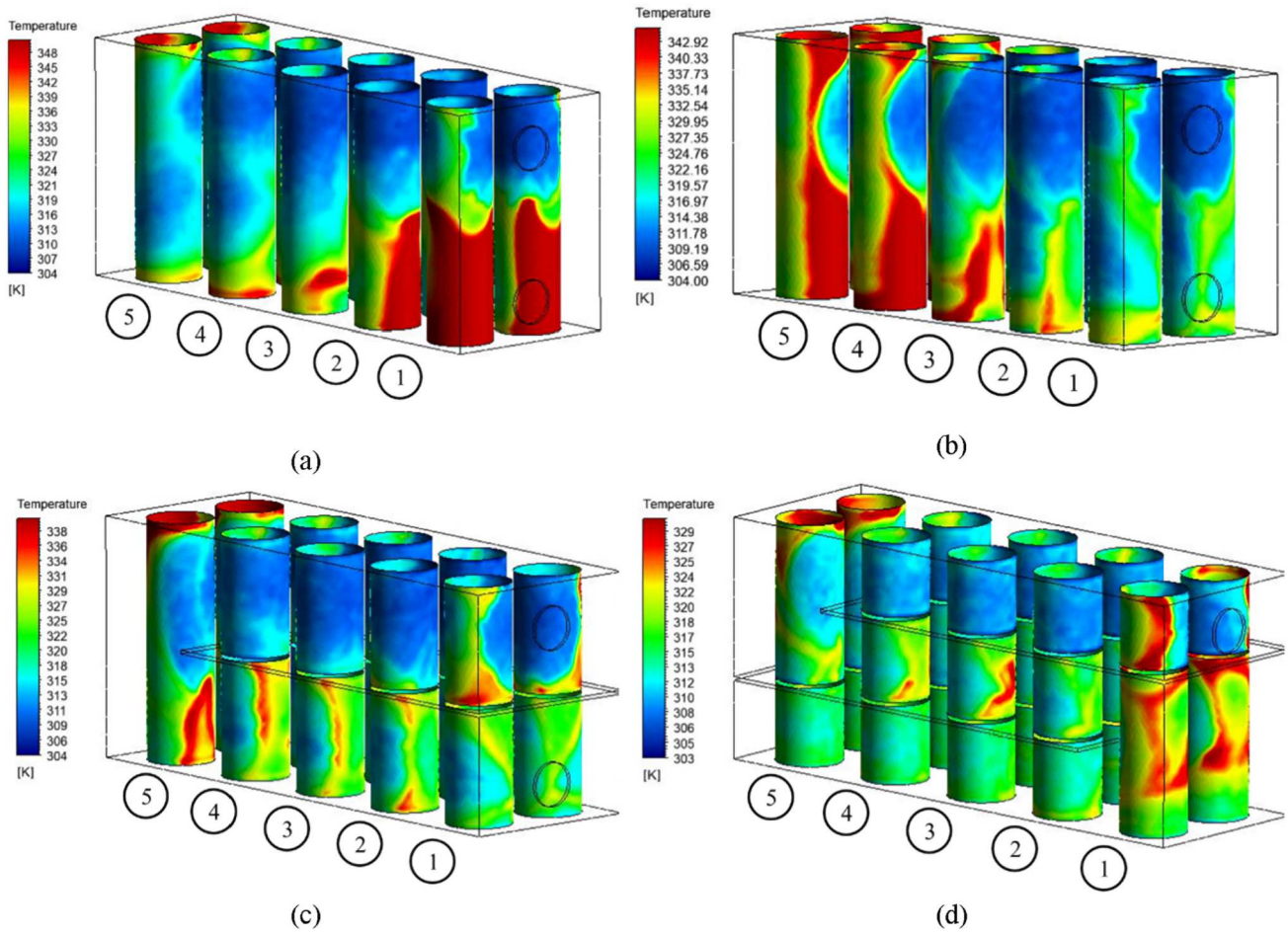

Figure 15. Temperature distributions on the battery surface with Re = 2000 and the Nf of (a) case 1, (b) case 2, (c) case 3, and (d) case 4, [54].

To predict the maximum and distributional temperatures in LIBs with and without a copper foam layer, Jongpluempiti et al. [59] employed both theoretical and experimental methods, using a channel flow setup with ferrofluid as the coolant. The test system consisted of a battery pack comprising sixty 18650 cylindrical Li-ion cells, each rated at 25.2 V and with a total capacity of 30 Ah. The addition of copper foam had a significant impact on the TMS. To maintain a uniform temperature across the LIB pack, the presence of copper foam enhanced coolant mixing at the copper surface and within the region of the flow channel where the foam sheet was positioned. This, in turn, improved heat transfer efficiency. The simulation results closely matched the experimental data, with average errors of 5.79% for Battery Model I (without copper foam) and 4.95% for Battery Model II (with copper foam). The maximum temperature reached 27.4°C in Model I and 26.3°C in Model II. As shown in Figure 16, the coolant temperature increases progressively along the flow path, moving away from the inlet port.

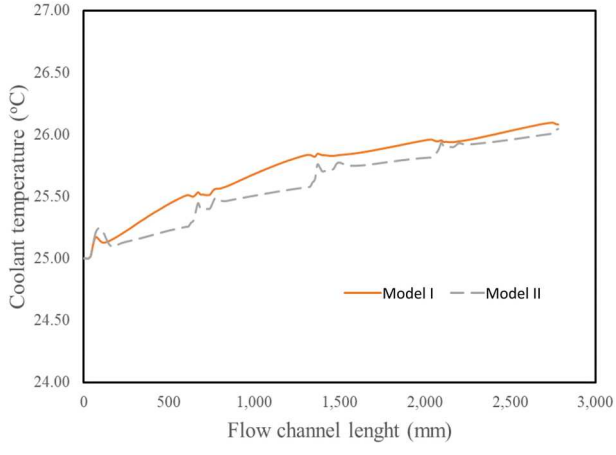

Figure 16. Coolant temperature variation as it passes through the cooling models [59].

Referring to the revised studies of Fe-nanofluids, Water-based Fe_2O_3 nanofluids overtook engine oil mixtures, while a hybrid nanofluid of nanodiamond and Fe_3O_4 accomplished a reduction in maximum

temperatures (23.1%) and temperature differentials (70.35%) at higher Re numbers. Also, it was indicated that nanoparticle mixing ratio and discharge rate have a notable effect on thermal performance, were the C-rate has the utmost effect on maximum temperatures. In this regard, optimal conditions hit a minimum temperature of 294 K. Also, integrating copper foam can enhance the heat transfer efficiency and improve the temperature uniformity in battery packs.

3.1.7. Nano-Newtonian-nanofluids

Alqaed et al. [60] investigated the behaviour of non-Newtonian nanofluids (NNfs) in a lithium-ion battery cooling system (Li-iBCS), which integrates a LIB with a solar-assisted cooling setup. A pouch-type lithium battery consists of three components: the anode, the cathode, and a capillary-integrated Li-iBCS. After the surfaces of the anode and cathode are cooled, a water-based carboxymethyl cellulose (CMC)/CuO NNF enters the system at a constant velocity and temperature and exits after heat absorption. The NNFs exhibit laminar flow characteristics, and the FEM was employed to solve the governing equations for fluid flow and heat transfer in the system. The study revealed that increasing the fluid velocity within the Li-iBCS reduces both the average battery temperature and the outlet fluid temperature. Moreover, increasing the volume percentage of NPs not only decreases the average battery temperature but also enhances the figure of merit (FOM) and the heat transfer coefficient. The highest FOM value of 1.36 was achieved at a velocity of 0.1 m/s with a nanoparticle volume concentration of 3%. Conversely, the lowest FOM value of 1.01 occurred at a velocity of 0.5 m/s and a nanoparticle volume fraction (VOP) of 0.5%.

In a separate study, Alnaqi [61] examined the thermal performance of a plate-type LIB pack composed of multiple individual cells. Nf flow channels were placed on both the left and right sides of each cell to facilitate effective cooling. A bionic design inspired by natural systems was employed to simulate the flow of NNfs through the embedded channels. The investigation into the LIB's thermal behaviour showed that incorporating NPs into the base fluid significantly reduces thermal resistance and improves surface temperature uniformity. This effect was consistent regardless of increases in fluid velocity. Additionally, increasing the velocity and volume fraction of NPs led to a reduction in the maximum battery temperature. However, this came with a considerable rise in pumping power – by 12.62 times for water and 14.53 times for nanofluids at a 3% volume fraction when the inlet velocity increased from 0.01 m/s to 0.05 m/s. At a velocity of 0.01 m/s and a nanoparticle volume fraction of 3%, the heat transfer coefficient increased by up to 14% compared to the base fluid under the same conditions.

To summarise the above studies of Nano-Newtonian-nanofluids, a water-based carboxymethyl cellulose (CMC)/CuO NNF can efficiently lessened average battery temperatures, with the highest figure of merit (FOM) of 1.36 attained at 0.1 m/s and 3% nanoparticle concentration. Also, integrating nanoparticles into a plate-type LIB pack can improve thermal resistance and surface temperature uniformity. However, higher velocities and nanoparticle concentrations can increase pumping power besides lowering maximum peak temperature of LIBs.

3.1.8. SiO_2-nanofluids

Hasan et al. [62] employed a novel cooling mechanism to reduce the temperature of LiB cells, operating within a Reynolds number range of 15,000–30,000. This was achieved by applying the Finite Volume Method (FVM) to solve the continuity, momentum, and energy equations. To analyse the thermal management of a system consisting of 52 LiB cells, the researchers used the CFD software ANSYS Fluent to simulate flow and temperature fields. The research examined the thermal behaviour of a water-based Nf containing dispersed SiO_2 NPs. The results indicated that, across all Re numbers evaluated, the Nf with the highest concentration of 5 vol.% SiO_2 exhibited the lowest average cell temperature. This enhanced cooling performance was attributed to improved thermal diffusion resulting from the increased effective thermal conductivity of the Nf. The findings support the use of a 5 vol.% SiO_2 Nf to optimise the cooling process. Increasing the Re number intensified turbulence within the flow, significantly improving heat transfer. Specifically, increasing the Re number from 15,000 to 22,500 and then to 30,000 resulted in a 32% and 65% increase in the Nusselt number, respectively. Overall, the use of nanofluids – particularly SiO_2-based formulations – demonstrated a significant enhancement in cooling performance, as illustrated in Figure 17.

A new cooling system for LIB packs using variable silicon dioxide (SiO_2) nanoparticle sizes was proposed by Hasan et al. [63] and analysed using CFD. The system employed a SiO_2–water Nf as the coolant. Across all Re numbers, the results showed that the average Nusselt number increased as the nanoparticle size decreased. This enhancement is attributed to the higher surface area of smaller NPs, which leads to a greater collision rate with the fluid molecules and, consequently, improved heat transfer. For nanoparticle sizes of 50, 40, 30, and 20 nm, the Nusselt number

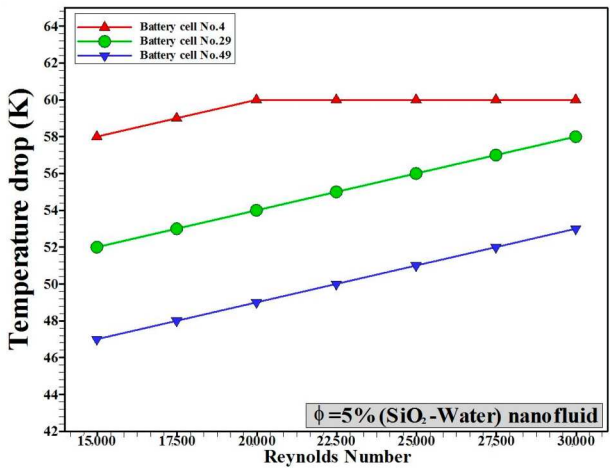

Figure 17. Temperature variation for battery cells at various Re (extraction) [62].

increased by 2.8%, 5.5%, 11.6%, and 22.6%, respectively. Additionally, at Re = 30,000, the temperature of Cell 4 was equal to the inflow temperature for all particle sizes. This outcome is due to the significant temperature difference between Cell 4 and the incoming coolant, resulting from Cell 4's position in the first column and its alignment with the inlet flow direction. Consequently, Cell 4 experienced greater heat dissipation to the coolant compared to other cells. The study demonstrated that improved heat exchange in LIB packs can be achieved by using smaller NPs and operating at higher Reynolds numbers.

According to the revised studies of SiO_2-nanofluids, it can be stated that a water-based nanofluid with 5 vol.% SiO_2 can reduce average cell temperatures and improve heat transfer, with an important increase in the Nusselt number as Re numbers rose. Also, smaller SiO_2 nanoparticles can enhance heat transfer efficacy as a result to their greater surface area.

3.1.9. Hybrid-nanofluids

An investigation aimed at improving the effectiveness of liquid cooling in cylindrical battery modules using hybrid nanofluids was conducted by Venkateswarlu et al. [64]. One promising approach to enhance heat transfer and thermal conductivity in battery cooling systems involves the use of hybrid nanofluids – mixtures composed of a base coolant fluid combined with NPs of different materials and concentrations. In this study, a hybrid Nf consisting of copper and aluminum oxide ($Cu + Al_2O_3$) dispersed in water (H_2O) was developed. Compared to conventional Al_2O_3/H_2O nanofluids, the $Cu + Al_2O_3/H_2O$ hybrid Nf demonstrated a 3.64% reduction in battery temperature due to enhanced thermal properties. However, due to the differing thermal characteristics of the two types of NPs, increasing the nanoparticle volume fraction in the hybrid Nf led to a 4.19% reduction in the heat transfer rate – occurring at a faster rate than with the Al_2O_3/H_2O Nf alone.

Thawkar et al. [65] investigated the efficiency of a TMS for EV LIBs using a helical coiled pulsing heat pipe (HC-PHP) and a hybrid Nf composed of Al_2O_3–multi-walled carbon nanotubes (MWCNT) in ethylene glycol. The experimental study focused on the performance of the system under various operating conditions. The HC-PHP system successfully maintained battery temperatures below 42°C during continuous discharge at room temperature (25°C) and discharge rates of 1C, 2C, and 3C, thereby keeping the battery within safe operating limits. Additionally, the internal temperature variation remained within 2°C, as indicated by the maximum temperature gradient across the battery. The system improved thermal uniformity across the battery surface and significantly reduced temperature gradients. As a result, the HC-PHP ensured optimal LIB performance by maintaining temperatures within the ideal range of 20–50°C, an essential factor for reliable and safe battery operation.

In their comprehensive study on LIBPs thermal management, Sheikholeslami et al. [66] aimed to enhance cooling efficiency through innovative design techniques. The researchers tested four different mini-channel configurations – Smooth (basic rectangular), Grooved, Tooth, and Pin Fin – using a hybrid Nf composed of water and Fe_3O_4–SWCNT (single-walled carbon nanotube) NPs. These advanced cooling channel designs were optimised to improve the system's thermal performance and regulate battery temperatures more effectively. The research employed a conduction-based model to simulate the transient heat generation conditions typically observed during battery discharge cycles. The results indicated that cells located near the cooling channels exhibited more uniform temperature distributions. Furthermore, the addition of NPs to the cooling fluid resulted in a modest reduction in battery temperature. Among the tested configurations, the Pin Fin channel significantly outperformed the Smooth rectangular duct, enhancing heat transfer performance by a factor of 5.03.

Figure 18 illustrates the mini-channel cooling block used in the numerical study conducted by Selvarajoo et al. [67]. The research examined the use of water and a hybrid Nf composed of Al_2O_3 and graphene oxide (GO) for thermal management of cylindrical 18650 LIBs. CFD simulations were used to evaluate the effects of fluid velocity, nanoparticle concentration, and discharge current on thermal performance. The thermal conductivity and dynamic viscosity of the Al_2O_3–GO hybrid Nf

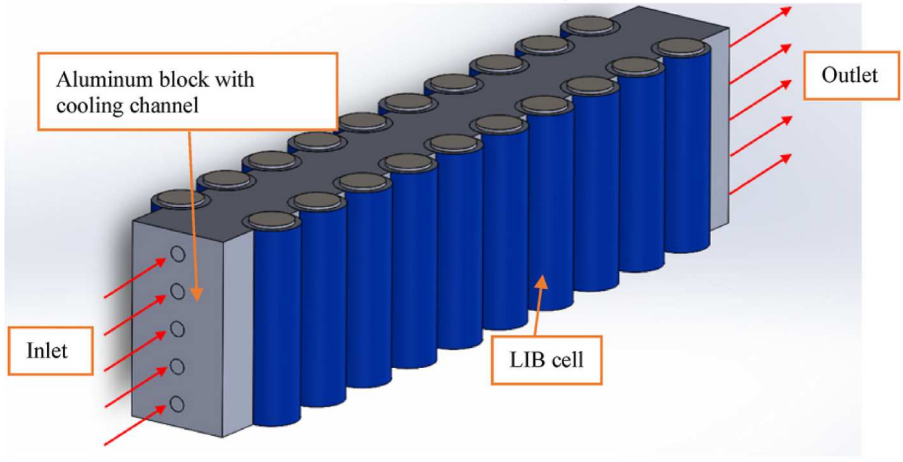

Figure 18. Design of cooling blocks using LIB [67].

were also experimentally analysed. An innovative cooling block design featuring 5 mm-diameter circular channels was developed and validated using experimental data, which showed a maximum temperature variation of just 0.26°C. Using a hybrid Nf with a 1.0 vol.% concentration improved thermal conductivity by 42.5% and reduced LIB cell temperatures by 7.47%. However, notable temperature variation among cells was still observed. Further cooling improvement of 7.53% was achieved by increasing the fluid velocity from 0.1 to 0.3 m/s. Due to their superior heat transfer properties, the study concluded that Al_2O_3–GO hybrid nanofluids are highly effective for BTMS, even under high discharge current conditions. As illustrated in Figure 19, the base fluid exhibited the lowest Nusselt number (Nu) at a 2C discharge rate, with values of approximately 6.52 and 7.67. In contrast, the highest Nu values achieved using a 1.0% Al_2O_3–GO Nf at velocities of 0.1 m/s and 0.3 m/s were 8.71 and 10.69, respectively.

In a summary, it can be ascertained that a hybrid nanofluid of copper and aluminum oxide (Cu + Al_2O_3) in water can achieve a 3.64% reduction in battery peak temperature in a comparison to conventional Al_2O_3 nanofluids. However, increasing the nanoparticle volume fraction led to a 4.19% reduction in heat transfer rate. Also, using a helical coiled pulsing heat pipe (HC-PHP) with an Al_2O_3-multi-walled carbon nanotube (MWCNT) hybrid nanofluid can maintain battery temperature below 42°C throughout discharge and lessening internal temperature variations to within 2°C. Finally, Al_2O_3-graphene oxide hybrid nanofluid for cylindrical LIBs can attain a 42.5% rise in thermal conductivity and a 7.47% reduction in cell temperatures at a 1.0 vol.% concentration.

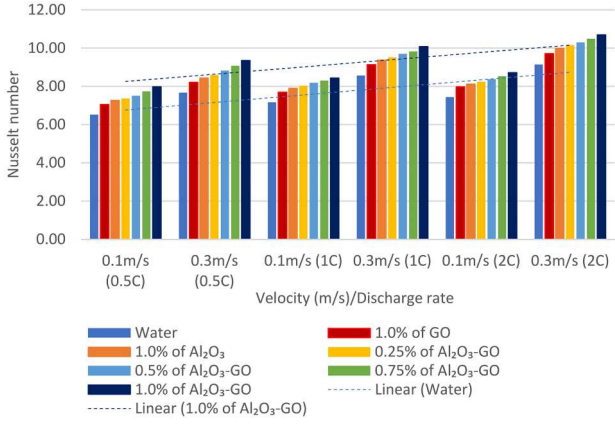

Figure 19. Nusselt number comparison [67].

3.1.10. Ternary hybrid-nanofluids

Kumar et al. [68] employed an electrochemical model for 3D battery thermal simulations. Using THNFs – specifically, THNF1 [Al_2O_3 (0.5%) + Cu (0.5%) + MWCNT (1%)/water] and THNF2 [Al_2O_3 (0.5%) + Cu (0.5%) + Graphene (1%)/water] – they investigated the effects of microchannel geometries (circular and rectangular cross-sections) at a discharge rate of 3C. The findings indicated that both the microchannel cross-sectional shape and the use of THNF significantly influenced thermal performance. Key performance metrics included the maximum and uniform cell temperatures, pump power consumption, and the ratio of heat transfer coefficient to pressure drop. The model demonstrated predictive capability for assessing thermal responses of batteries during charge and discharge cycles. With THNF2, the proposed system successfully reduced the temperature of a 26,650-type cylindrical cell to 305.24 K while maintaining a temperature differential of just 5.23 K. Additionally, microchannels with rectangular cross-sections outperformed their circular counterparts in terms of thermal

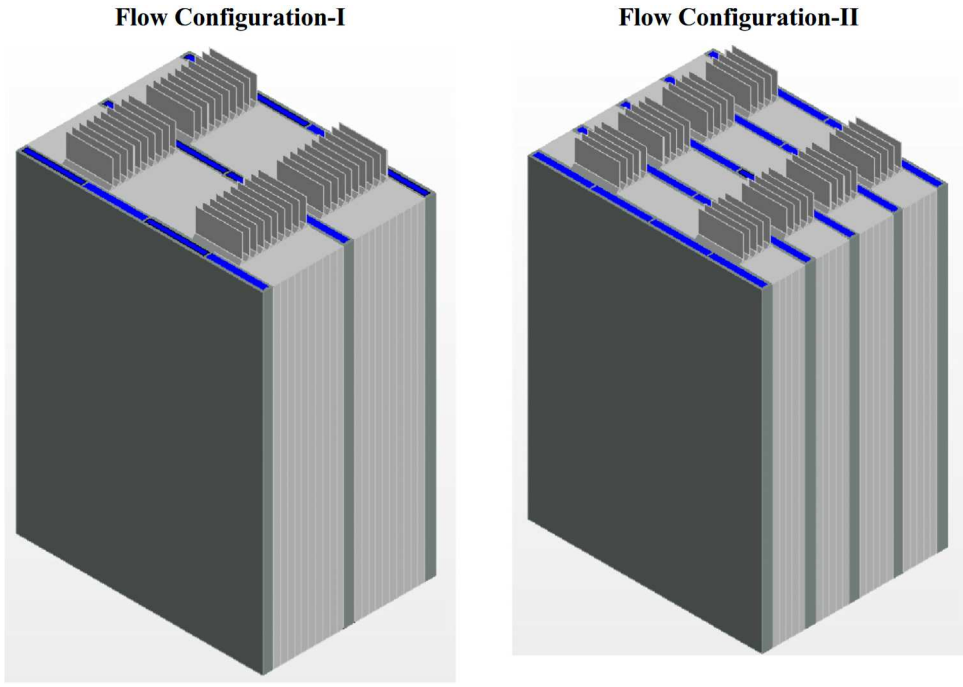

Figure 20. Battery module variants [70].

regulation. Overall, the use of THNF significantly improved battery temperature control.

Liu et al. [69] tested and implemented a ternary hybrid Nf composed of Al_2O_3–TiO_2–CuO as a cooling medium to enhance the performance of a liquid-cooled BTMS. At room temperature, this Nf exhibited a 42.7% improvement in thermal conductivity with a nanoparticle mass fraction (NMF) of 0.75% and a composition ratio of Al_2O_3:CuO:TiO_2 = 0.8:0.1:0.1. A surfactant – sodium dodecyl benzene sulfonate (SDBS) – was used in a mass ratio of 0.2 g SDBS per gram of NPs to ensure colloidal stability. However, the viscosity of the Nf increased by 17.3%. Simultaneously, a 97-cell (18650) battery module featuring a wave-shaped cooling tube with a variable cross-section was developed to study the impact of NMF on thermal performance during high-rate discharge. Results showed that, compared to pure water cooling, a 0.75% NMF Nf reduced the maximum battery module temperature by 9.8% and decreased the temperature differential by 22.3%. Furthermore, all thermal management requirements were met with a coolant velocity of 0.15 m/s, enabling effective cooling with minimal power consumption at the optimal NMF of 0.75%.

To sum up, it can be said that THNFs with Al_2O_3, Cu, and MWCNT or graphene can be utilised to reduce the peak temperature of a cylindrical cell to 305.24 K with a minimal differential of 5.23 K. A hybrid nanofluid of Al_2O_3, TiO_2, and CuO,can attain a 42.7% rise in thermal conductivity at a 0.75% nanoparticle mass fraction. In turn, this enables to reduce the maximum battery temperature by 9.8% and the temperature differential by 22.3% in a comparison to pure water cooling.

3.1.11. Different types of nanofluids

As a heat transfer fluid for active thermal management, Mondal et al. [70] proposed the use of nanofluids – colloidal suspensions of NPs in a base fluid. To evaluate the effectiveness of nanofluids for thermal management in LIBs, the researchers examined two flow configurations and two types of nanofluids (ethylene glycol–water + Al_2O_3 and Al_2O_3–water) to assess their impact on temperature distribution within standard battery modules (Figure 20). The objective of the study was to address EV specific design challenges, battery performance, and heat dissipation capabilities under conditions of high ambient temperatures and elevated discharge rates. Figure 21 presents the span-wise average coolant temperature distribution along the flow direction, from inlet to outlet, at the end of a 5C discharge for flow configuration I (FC-I), under three different inlet velocities. At the lowest velocity of 0.01 m/s, the coolant remains in the channel for a longer duration, resulting in a temperature increase of over 18°C between the inlet and outlet. The coolant used in this case is based on an ethylene glycol (EG)–water mixture.

Using a three-dimensional CFD model, Liu et al. [71] quantitatively investigated a mini-channel cooling system for the thermal management of high-power prismatic batteries. The thermal performance of the cooling

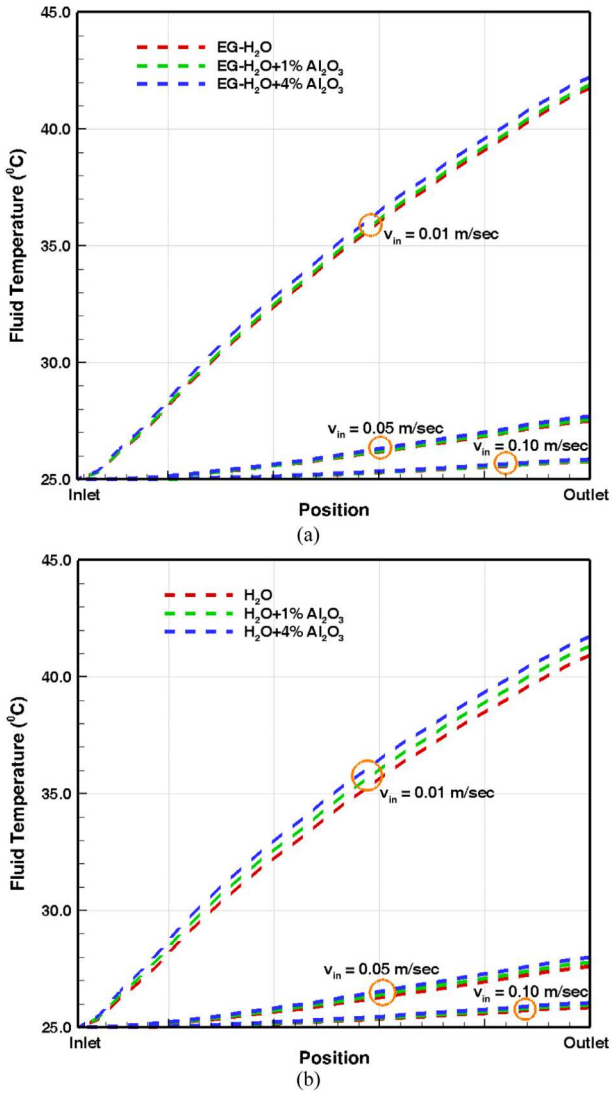

Figure 21. Coolant temperature increase along channel length following a 5C discharge for (a) EG-H_2O and Al_2O_3 and (b) H_2O and Al_2O_3 [70].

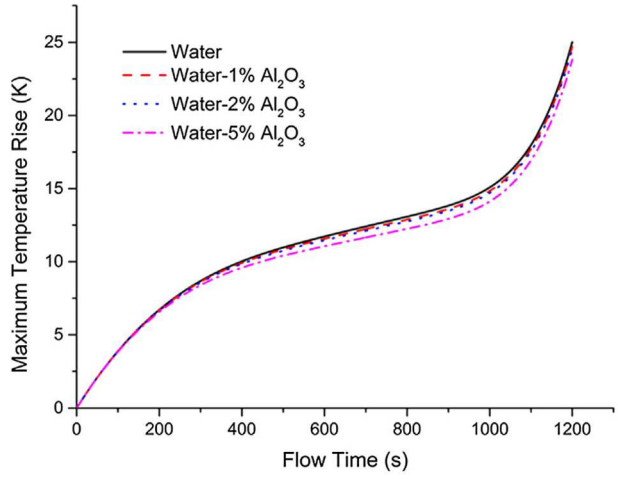

Figure 22. Impact of the volume percentage of NPs on the highest temperature increase [71].

system was evaluated using different base fluids, such as water, engine oil, and ethylene glycol, as well as their corresponding nanofluids used as coolants. A semi-empirical correlation was employed to estimate the thermal conductivities of the nanofluids, while experimental data were used to fit curves representing the dynamic viscosities of nanofluids with various base fluids. Among the base fluids tested, water exhibited the best cooling performance due to its high thermal conductivity. However, for fluids with lower thermal conductivity, such as engine oil, the addition of NPs had a more pronounced effect on enhancing heat transfer. Overall, the cooling performance of nanofluids surpassed that of pure water, thermal performance improved with increasing nanoparticle volume fraction (Figure 22). Figure 23 further illustrates that using a water-based Nf with 5% Al_2O_3 reduced the maximum temperature rise in Cell 1 by 1.24 K and in Cell 3 by 1.20 K.

Kiani et al. [72] developed a novel BTMS that integrated a magnetic field, a metal foam–paraffin PCM composite, Nf cooling, and a heat sink. To experimentally replicate the heat generated by a battery, a surrogate battery model was used. The primary performance metric was the prevention of thermal runaway. At a Re of 1250, the system's operational duration improved by 179%, and the maximum battery temperature was reduced by 7.5°C compared to the baseline case. Similarly, at Re = 890, battery cooling performance improved by 151%. The proposed hybrid BTMS also significantly reduced the temperature differential, maintaining it below 4°C. Experimental results demonstrated that the hybrid BTMS effectively dissipated both generated and stored heat, significantly lowering battery temperatures and enhancing system reliability. To assess the thermal performance of the LIB, three different volume fractions of metallic NPs were evaluated. As illustrated in Figure 24, both the maximum temperature and its progression decreased as the concentration of metallic NPs increased – an expected outcome given their superior thermal conductivity.

Liao et al. [73] proposed the use of Nfs with high thermal conductivity as coolants and evaluated several types for their effectiveness in cooling batteries compared to water. Among the tested fluids, a copper (Cu) water-based Nf demonstrated the best performance, reducing the maximum battery temperature by 1.066 K and the maximum temperature differential of the battery pack by 12.6% compared to water. Subsequent analysis focused on how different Nf parameters affect

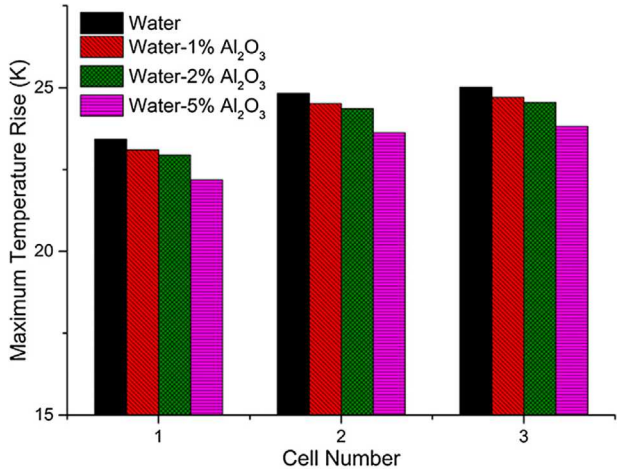

Figure 23. Changes in the maximum temperature increase [71].

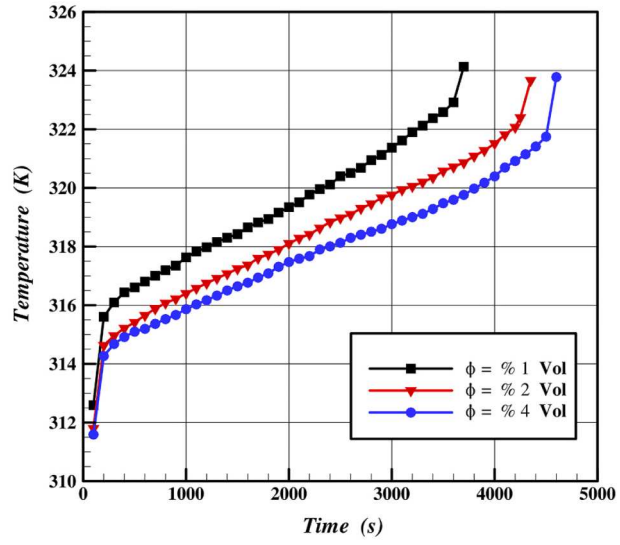

Figure 24. Temperature change over time for varying amounts of Nf [72].

the thermal performance of BTMS. The findings indicated that as the pressure drop, Nf volume fraction, and flow velocity increased, both the maximum battery pack temperature and temperature differential decreased. Notably, reducing the nanofluid's inlet temperature led to an impressive 10 K reduction in the maximum battery temperature. However, this also negatively impacted temperature uniformity, resulting in a maximum temperature differential of 8.333 K.

Hasan et al. [74] employed an innovative cooling mechanism to reduce cell temperatures in a battery pack, operating at Re ranging from 1,500 to 3,000. The cooling system used water as a base fluid, with 5% concentrations of NPs (Al_2O_3, CuO, SiO_2, and ZnO), each with an average particle diameter of 20 nm. The results showed that the Nusselt number (Nu) increased with rising Re. In the 52-cell battery pack, circulating Nf

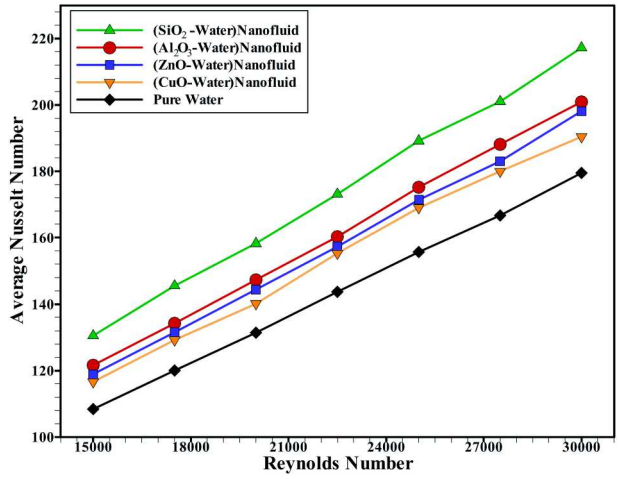

Figure 25. Nusselt number (Nu) average employing various Nf types at various Reynolds numbers [74].

between the cells effectively lowered the temperature of the Li-ion cells. Although higher Re values slightly increased pumping power requirements, SiO_2 nanofluids at Re = 18,000 offered the best thermal performance. Among all nanofluids tested, SiO_2 demonstrated the highest cooling efficiency, followed closely by Al_2O_3 and ZnO nanofluids. The temperature reductions of the hottest battery cell were observed to be >47°C, 44°C, 43°C, 42°C, and 42°C for SiO_2, Al_2O_3, ZnO, CuO nanofluids, and pure water, respectively. Figure 25 shows that the Nu values for SiO_2 nanofluids are higher than those for Al_2O_3 nanofluids. Figure 26 further illustrates the effective cooling process, indicating that the average battery temperature ranged between 302 K and 308 K, depending on the Re number.

Venkateswarlu et al. [75] investigated the heat transfer performance of a cylindrical battery module using nanofluids in a liquid cooling system. A 50:50 ethylene glycol–water (EG-water) mixture was used as the base fluid, combined with two different nanofluids (NFs): CuO/EG-water and Al_2O_3/EG-water. The researchers employed numerical methods to solve the governing ordinary differential equations (ODEs) by integrating the shooting method with the Runge-Kutta-Fehlberg technique. Both two-dimensional and three-dimensional models were used to analyse temperature distributions, velocity fields, drag forces, and heat transfer (HT) rates. The researchers examined Nf flow around a cylindrical LIB cell, including detailed velocity and temperature profiles, fractional drag forces, and heat transfer rates. The results showed that increasing the nanoparticle volume fraction led to temperature rises of 36.52% for Al_2O_3 and 44.20% for CuO nanofluids. Due to their distinct thermophysical properties, CuO/EG-water nanofluids reached their peak temperature 7.68%

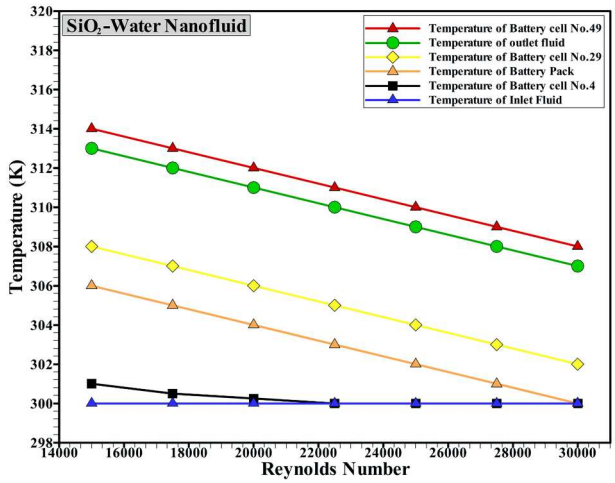

Figure 26. Temperature distribution variation utilising SiO_2 Nf as a cooling fluid at various Reynolds numbers [74].

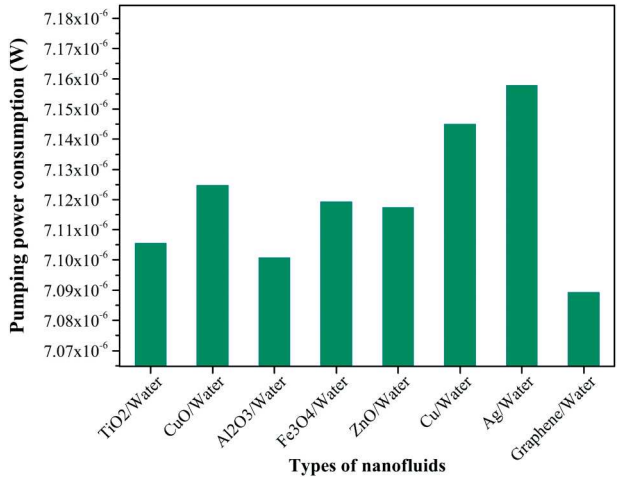

Figure 27. Power consumption of pumps for different types of nanofluids [76].

faster than Al_2O_3/EG-water nanofluids. Under negative heat flux conditions ($Q < 0$), CuO/EG-water nanofluids became 56.47% hotter, while Al_2O_3/EG-water nanofluids were 16.30% cooler. NPs also significantly enhanced thermal performance: heat transfer improved by 50.17% and 57.38%, while drag force increased by 45.36% and 47.04% for Al_2O_3 and CuO nanofluids, respectively. Overall, the heat transfer performance of CuO/EG-water nanofluids was found to be 8.20% greater than that of Al_2O_3/EG-water nanofluids.

An investigation into the development and application of mono- and hybrid nanofluids to enhance the cooling performance of 18650 LIBs was conducted by Kanti et al. [16]. The study began by dispersing Al_2O_3 and CuO NPs in water at a volume concentration of 0.5% to create advanced coolant formulations. Battery cooling efficiency was evaluated under various conditions using an experimental setup. The variables included coolant type, flow rates (150, 250, and 350 ml/min), and battery discharge rates (0.5C and 1C). At 60°C, the thermal conductivity of the Al_2O_3–CuO hybrid Nf was 35.26% higher than that of the CuO monofluid and 29.1% higher than that of the Al_2O_3 monofluid. Compared to pure water, the 0.5% Al_2O_3–CuO Nf significantly reduced LIB cell temperatures by 54.23% at a flow rate of 350 ml/min.

Moayedi [76] evaluated eight different nanofluids for use as liquid coolants in a 14.6 Ah LIB. The effects of key parameters, including Nf type, volume fraction, ambient temperature, and convective heat transfer coefficient, on LIB thermal performance, pumping power consumption, temperature deviation, and maximum cell temperature were investigated using three-dimensional numerical simulations. The results showed that employing nanofluids could reduce the maximum LIB temperature by 26.46 K (from 321.69 K to 295.23 K), maintaining it within a safe operating range compared to a system without liquid cooling. Enhancements in LIB operation and lifespan were achieved by decreasing the maximum temperature by 0.22 K and 0.09 K, and by reducing temperature deviation by 14.71% and 2.98% through increases in the nanofluids' convective heat transfer coefficient and volume fraction, respectively. From the perspectives of pumping power usage, thermal performance, and temperature uniformity, the Graphene/Water Nf emerged as the most promising coolant among the eight Nf candidates, as seen in Figure 27.

Deng et al. [77] investigated the cooling performance and critical suppression capability of spray cooling in mitigating thermal runaway (TR) in LIBs using three different nanofluids: boron nitride, titanium dioxide, and aluminum oxide – each dispersed in distilled water at a fixed concentration of 0.1 vol.%. The researchers demonstrated that nanoparticle-infused water mist can significantly accelerate the cooling process. Compared to pure water mist, nanofluid-based mist reduced the cooling time by 46%, requiring only 11 s to bring the temperature down from its peak during thermal runaway to below 100°C. The maximum cooling rate achieved with Nf spray was 127.4°C/s, surpassing that of water mist by 61.29%. Furthermore, to prevent thermal runaway at elevated temperatures, Nf sprays were able to raise the critical suppression temperature by up to 40°C, compared to the 160°C threshold of water mist. The maximum heat dissipation rate achieved by Nf sprays was 6067.4 W.

Referring to the relevant studies of different types of nanofluids, it can be said that ethylene glycol-water mixtures with Al_2O_3 can demonstrate over 18°C temperature

rises at low flow velocities. In this regard, lower thermal conductivity fluids promoted more from the integration of nanoparticles, enhancing heat transfer. A hybrid thermal management system using nanofluids and metal foam can notably reduce the maximum peak battery temperatures by 7.5°C, enhancing safety metric. Also, copper-water nanofluids can lowere the maximum battery temperatures by 1.066°K in a comparison to water, with higher nanoparticle concentrations further improving performance. SiO_2 nanofluids obtained the greatest cooling efficacy, reaching drops of over 47°C in the hottest battery cell. CuO nanofluids also knowingly enhanced heat transfer, decreasing peak temperatures faster than Al_2O_3. An Al_2O_3–CuO hybrid nanofluid augmented thermal conductivity by 35.26% and lessened LIB cell temperatures by 54.23% at optimal flow rates. The graphene-water nanofluid verified to be most active, reducing maximum LIB temperatures by 26.46°K. Finally, nanofluid sprays attained an inspiring cooling rate of 127.4°C/s during thermal runaway, meaningfully growing critical suppression temperatures. Table 1 provides a summary of published studies on the application of nanofluids in LIB TMSs that do not involve PCMs.

3.2. Nanofluids in lithium-ion batteries with PCM

3.2.1. Aluminium-nanofluids

Using a novel TMS that combines both active and passive cooling methods, Mashayekhi et al. [78] investigated the thermal response of LIBs under high discharge rates. The passive component of the TMS consisted of block-form paraffin (P 42–44 #107150) embedded in a porous copper metal foam. The active component was an aluminum mini-channel designed to carry coolant flow. The study was conducted under both active and hybrid cooling configurations at three different Re. The results showed that the maximum battery temperature decreased with increasing flow rates. However, passive cooling alone was ineffective in reducing the battery temperature below the critical safety limit of 60°C during rapid discharge. In comparison to the active-only method, the hybrid system successfully reduced the steady-state battery temperature by 19.5% at Re = 340 and a heat generation rate of 3.7 W. Additionally, the effects of using two different volume fractions of Al_2O_3–water nanofluids were evaluated in both active and hybrid systems. In the active approach, nanofluids lowered the maximum battery temperature by 15.5% compared to the baseline water-cooling case, while in the hybrid configuration, the reduction was 8.5%.

Kiani et al. [79] developed a hybrid TMS by incorporating an active cooling loop using alumina Nf and a passive system consisting of copper foam saturated with paraffin as the PCM. The results demonstrated that this hybrid cooling strategy could ensure battery safety under demanding operating conditions, irrespective of heating power or Re number. Under high discharge rates, it was assumed that the PCM had fully transitioned to the liquid phase at the onset of critical conditions. At 41 W heating power and Re = 420, the onset time of thermal stress increased from 3700 s with a 1 vol.% Nf to 4600 s with a 2 vol.% nanofluid. At Re values of 420 and 400, using 1 and 2 vol.% nanofluids extended the operational time of the battery by 200 and 900 s, respectively, compared to a water-based cooling system. Replacing water with nanofluids effectively delayed the initiation of paraffin melting, thereby extending the melting duration and reducing the rate of temperature increase – an essential factor in improving battery safety and performance under high thermal loads.

Jiang et al. [80] employed two methods to manage the temperature of a battery pack: passive cooling using PCMs and active cooling using forced Nf flow. The LIB pack was cubical in shape and comprised cylindrical cells, with the entire cube volume filled by the PCM. Inside the battery pack, the Nf flowed through a helical tube. A Nf composed of water, boehmite, and alumina, with various nanoparticle morphologies, was used. By varying the Nf velocity, several parameters were quantitatively investigated, including battery temperature and the heat transfer coefficient (HTC). The Nf flow within the pack was modelled using COMSOL Multiphysics. Among the different nanoparticle morphologies tested, blade-shaped particles resulted in the greatest reduction in both maximum temperature and the volume of molten PCM at different time intervals. When the Nf velocity was increased from 0.02 to 0.06 m/s, the amount of molten PCM decreased by 4.7%, while the Nf HTC increased by 70%. This velocity increase also reduced the outlet Nf temperature by 0.44°C and lowered the maximum and average battery temperatures by 1.24°C and 1.53°C, respectively.

Jiang et al. [81] statistically evaluated the cooling of a cubic battery pack consisting of nine cylindrical LIB cells. The pack was initially fitted with three independent ducts carrying alumina (Al_2O_3)/water Nf. The entire assembly, including the battery cells and ducts, was then submerged in a PCM. The influence of nanoparticle volume fraction and duct height on thermal performance was analysed via simulations. The experiment, conducted over a 60,000-second interval, measured the volume of molten PCM, Nf and battery temperatures, and the overall heat transfer coefficient (U-value) for both materials. A maximum of 67.5% of the PCM

Table 1. A summary of the associated studies related to the nanofluids in LIBs without PCM.

The researchers (year) [reference]	Nanofluid composition	Nanofluid concentration	Results and remarks
Al_2O_3-nanofluids			
Sefidan et al. (2017) [28]	Al_2O_3-water nanofluid.	$0 \leq \ \leq 0.06$	The increase in thermal conductivity for greater volume fractions is responsible for the observed decrease in maximum temperature over simulation time as the volume fraction increases.
Sarchami et al. (2022) [29]	Al_2O_3-water nanofluid.	$0 \leq \phi \leq 0.06$	Compared to DI water, the peak discharge temperature was 1.2°C lower and the temperature differential was 0.4°C smaller when a 2% volume fraction of Alumina Nf was used.
Sarchami et al. (2022) [30]	Al_2O_3-water nanofluid.	$0.01 \leq \phi \leq 0.02$	As the concentration of alumina NPs in the deionised water was enlarged, the maximum temperature and the temperature differential were significantly decreased.
Liu et al. (2023) [31]	γ-Al_2O_3-water nanofluid.	$0 \leq \phi \leq 0.02$	Under ideal conditions, the battery module would be cooled by 0.24, 0.31, and 0.52°C, respectively, and the cooling performance would be improved by 3.77%, 5.02%, and 8.16% with a flow rate of 0.9 L/min and a concentration of 0.1%, 1%, and 2% of γ-Al_2O_3/heat transfer fluid nanofluid, respectively.
Wang et al. (2023) [32]	Al_2O_3-water nanofluid.	$0 \leq \phi \leq 0.1$	The heat transfer is increased by 12.1% and the formation of thermal and viscous entropy is decreased by 5.37% and 23.2%, respectively, when the volume percentage of the current Nf is increased to 0.1%.
Anqi (2023) [33]	Al_2O_3-water nanofluid.	$0 \leq \phi \leq 0.1$	Up to 20% more heat may be transferred from the serpentine microchannel to the battery when using Nf.
Ouyang et al. (2023) [34]	Al_2O_3-water nanofluid.	$0 \leq \phi \leq 0.03$	There is a 23% drop in maximum battery temperature and a 22% drop in economic index in the revised plan when compared to plan 6.
Jha et al. (2024) [35]	Al_2O_3-water nanofluid.	$0 \leq \phi \leq 0.01$	Five 6-millimeter-wide channels etched into the aluminum cold plate, with a coolant of 1% Al_2O_3 in a 20:80 ethylene glycol-water nanofluid, provide the optimal thermal performance.
Banerjee and Nidhul (2025) [36]	Al_2O_3-water nanofluid.	$0 \leq \phi \leq 0.01$	When using Nf as a cooling agent, the amount of power required to pump the fluid is minuscule in comparison to the power output from the battery pack.
Cu-nanofluids			
Wu and Rao (2017) [37]	Cu-water nanofluid.	$0 \leq \phi \leq 0.06$	Enhanced natural convection significantly raised the heat transfer intensity when the Rayleigh number varied between 10^4 and 10^6.
Zhao et al. (2024) [38]	CuO-water nanofluid.	$0 \leq \phi \leq 0.04$	At Re = 60, a 4% increase in volume fraction resulted in a 2.19, 2.26, and 2.64°C decrease in maximum temperature for LIBP 1, 2, and 3, respectively.
Qawasmeh et al. (2024) [39]	CuO-water nanofluid.	$0.05 \leq \phi \leq 0.30$	The effect of NPs on thermal performance was demonstrated by the 9.46% drop in temperature.
TiO_2-nanofluids			
Chen and Li (2020) [40]	TiO_2-based nanofluid.	$0 \leq \phi \leq 0.02$	Within the specified temperature range of 20°C to 50°C, the TiO2-PHP guarantees that the LIB operates well.
Wiriyasart et al. (2020) [41]	TiO_2-based nanofluid.	0.25 and 0.50	The cooling capacity is increased when using nanofluids as a coolant rather than water.
Saghir et al. (2023) [42]	TiO_2-water nanofluid.	$0.1 \leq \phi \leq 0.5$	Adding metallic NPs (i.e. nanofluid) to water might improve its performance as a cooling liquid. Although the pressure loss is increased, the heat augmentation is 12% when Nf is used.
Saghir and Bicer (2023) [43]	TiO_2 nanofluid.	$0.001 \leq \phi \leq 0.005$	Ammonia was determined to be the most effective cooling fluid out of all the fluids tested, which included water, isopropanol, a binary combination of ammonia and water, and a Nf of titanium dioxide.
Carbon-nanofluids			
Yang et al. (2021) [44]	CNTs-water nanofluid.	$0 \leq \phi \leq 0.005$	The performance and efficiency of the battery may be improved by adding carbon nanotubes to the base fluid and then employing the nanofluids in microchannels to cool it.
Aberoumand et al. (2021) [45]	GO-vanadium electrolyte nanofluid.	$0.02 \leq \phi \leq 0.1$	There was a 12% improvement in electrical conductivity and a 4% improvement in thermal conductivity, both of which have the potential to improve the performance of flow batteries.
Zhou et al. (2021) [46]	CNT nanofluids.	$0.05 \leq \phi \leq 0.5$	The average evaporator temperature of the OHP was able to be decreased to 43.1°C and the thermal resistance to 0.066°C/W at a CNT concentration of 0.2 wt.%.
Kim and Park (2021) [47]	CNT nanofluids.	$0 \leq \phi \leq 0.5$	The excellent mass transport capabilities of the nanofluids make them ideal for reducing concentration loss.
Aberoumand et al. (2023) [48]	rGO nanofluidic.	$0 \leq \phi \leq 0.1$	Electrolytes with 0.1 wt.% Nf had a polarisation effect and reduced ohmic resistance.
Mitra et al. (2023) [49]	MWCNT-water nanofluid.	$0.15 \leq \phi \leq 0.45$	With 0.45% MWCNTs, the pressure drop is 13% more than water in the single-channel case and 14% greater in the dual-channel case.
Rana et al. (2024) [50]	MWCNTs-based nanofluids	$0.0015 \leq \phi \leq 0.0045$	More channels, higher nanoparticle concentrations, and different flow topologies all lead to better cooling performance.
Silver-nanofluids			
Tousi et al. (2021) [51]	AgO nanofluid.	$0.01 \leq \phi \leq 0.04$	The temperature differential and maximum temperature of the battery pack were kept below 1.07 and 305.59 K, respectively, when the liquid cooling system was run with a 7C discharge rate, optimum inflow velocity, and Nf volume % as the coolant.

(*Continued*)

Table 1. Continued.

The researchers (year) [reference]	Nanofluid composition	Nanofluid concentration	Results and remarks
Jahanbakhshi et al. (2022) [52]	Silver-water/ethylene glycol nanofluid.	$0 \leq \phi \leq 0.04$	The system's entropy production is improved with an increase in Re and φ.
Azizi et al. (2022) [53]	Ag-water nanofluid.	$0.001 \leq \phi \leq 0.008$	The most efficient example is the 0.8 wt.% Nf at Re = 850, which has an experimentally measured thermal performance factor (TPF) of around 1.35 and is expected to improve the Nusselt Number by about 67.1% when compared to the base liquid.
Rahmani et al. (2023) [54]	AgO-water nanofluid.	$0 \leq \phi \leq 0.03$	The Nusselt number can be improved by more than 25% by topological adjustments, and by no more than 30% by a rise in the Reynolds number from 1000 to 2000.
Rahmani et al. (2023) [54]	AgO-water nanofluid.	$0 \leq \phi \leq 0.03$	While the Reynolds number can grow by up to 30% between 1000 and 2000, topological adjustments can enhance the Nusselt number by over 25%.
Sarchami et al. (2024) [55]	AgO-water nanofluid.	$0 \leq \phi \leq 0.04$	Maximum temperature and temperature difference were both decreased by 3.08% and 60.7%, respectively, when 4% VF AgO-based Nf was used instead of DI-water.
Fe-nanofluids			
Yetik and Karakoc (2022) [56]	Fe2O3 nanofluids.	$0.03 \leq \phi \leq 0.06$	By increasing the volume fraction ratio from 3% to 6% with water as the refrigerant, the temperature of the battery model changed by 0.05 K. With EO as the refrigerant, the change was 1.15 K.
Dilbaz et al. (2022) [57]	ND- Fe_3O_4 W/EG hybrid nanofluid.	$0 \leq \phi \leq 0.02$	A 2% volume ratio of ND-Fe3O4 + W/EG hybrid Nf at 800 Re number improves the maximum temperature by 23.1% and the temperature differential by 70.35% contrasted to water with the same Re.
Yetik et al. (2023) [58]	Fe_3O_4-engine oil nanofluid.	$0 \leq \phi \leq 0.05$	The environment must be 283 K, the mixing ratio must be 5, the C-rate must be 2, and the inflow velocity must be 0.04 m/s in order to achieve the lowest possible maximum battery temperature.
Jongpluempiti et al. (2025) [59]	Fe3O4-water nanofluid.	$0 \leq \phi \leq 0.04$	The temperature of the coolant rises with the movement away from the inlet port.
Nano-Newtonian-nanofluids			
Alqaed et al. (2022) [60]	Water-CMC/CuO NNFs.	$0 \leq \phi \leq 0.04$	The av. temperature of the battery and the fluid's temperature upon exit are both lowered by raising the Li-iBCS's fluid velocity.
Alnaqi (2022) [61]	NN-Nfs.	$0 \leq \phi \leq 0.04$	By including 3% NPs at a velocity of 0.01 m/s, the heat transfer coefficient may be increased by a maximum of fourteen percent as contrasted to the pure fluid under the same circumstances.
SiO_2-nanofluids			
Hasan et al. (2023) [62]	SiO_2-water nanofluid	$0 \leq \phi \leq 0.05$	The av. temperature values at all Re tested were lowest for SiO_2 Nf with the largest volume fractions of 5%.
Hasan et al. (2025) [63]	SiO_2-Water Nanofluid.	$0 \leq \phi \leq 0.04$	The capacity of LiB cells to transfer heat is greatly enhanced by using smaller NPs and increasing the Reynolds number.
Hybrid-nanofluids			
Hai et al. (2024) [64]	Cu + Al_2O_3/H_2O hybrid nanofluid.	$0 \leq \phi \leq 0.05$	Because to the thermal main changes in both liquids, increasing the nanoparticle volume fraction in Cu + Al2O3/H2O hybrid nanofluids lessens the heat transfer rate by 4.19% at a faster rate than in Al_2O_3/H_2O nanofluids.
Thawkar et al. (2024) [65]	Hybrid nanofluid of Al_2O_3–MWCNT–ethylene glycol.	$0 \leq \phi \leq 0.04$	Crucial for the lithium-ion battery's dependable functioning, the HC-PHP keeps temperatures within the ideal range of 20–50°C, ensuring optimal performance.
Sheikholeslami et al. (2025) [66]	Fe_3O_4-SWMCT hybrid nanofluid.	$0 \leq \phi \leq 0.04$	Cells close to the cooling channels show a more consistent temperature distribution, and the battery temperature is somewhat reduced as a result of the NPs in the cooling fluid.
Selvarajoo et al. (2025) [67]	Al_2O_3-GO-based hybrid nanofluids.	$0 \leq \phi \leq 0.01$	The improved heat transfer characteristics of Al_2O_3-GO hybrid nanofluids make them ideal for BTMS, even while operating at high current discharge rates.
Ternary hybrid-nanofluids			
Kumar et al. (2024) [68]	Al_2O_3 + Cu + MWCNT /water and THNF2 (Al_2O_3 + Cu + Graphene /water].	0.005, 0.005, and 0.01, respectively.	Using ternary hybrid Nf significantly improves battery temperature regulation.
Liu et al. (2025) [69]	Ternary hybrid nanofluid of Al_2O_3-TiO_2-CuO.	$0 \leq \phi \leq 0.01$	When compared to pure water cooling, 0.75% NMF Nf cooling reduces the max. temperature within the module by 9.8% and lowers the temperature differential by 22.3%.
Different types of nanofluids			
Mondal et al. (2017) [70]	EG-water + Al_2O_3, Al_2O_3-water nanofluids.	$0.01 \leq \phi \leq 0.04$	Since the coolant spends longer time in the channel at a low velocity of 0.01 m/s, its temperature increased by more than 18 C between the intake and the outlet. The coolant is based on an EG-H2O combination.
Liu et al. (2018) [71]	Al_2O_3-EG, Al_2O_3-EO nanofluids.	$0 \leq \phi \leq 0.05$	When compared to pure water, nanofluids exhibit superior cooling characteristics, and this advantage grows as the particle volume percent increases.
Kiani et al. (2021) [72]	CuO and Fe3O4, nanofluids.	$0.01 \leq \phi \leq 0.4$	At Re = 1250, the system's operating duration is improved by 179%, and the max. battery's temperature is lowered by approximately 7.5°C contrasted to the basic case.

(*Continued*)

Table 1. Continued.

The researchers (year) [reference]	Nanofluid composition	Nanofluid concentration	Results and remarks
Liao et al. (2022) [73]	Al_2O_3, SiO_2, TiO_2, CuO and Cu-water nanofluid.	$0 \leq \phi \leq 0.04$	As the volume percentage and flow velocity of nanofluids grow, the maximum temperature difference and battery pack temperature both decrease. However, the pressure drop increases in direct proportion to these changes.
Hasan et al. (2023) [74]	Al_2O_3, CuO, SiO_2, and ZnO-water nanofluids.	$0.01 \leq \phi \leq 0.10$	The hottest battery cell's temperature decrease grasps >47, 44, 43, 42, and 42°C for SiO_2 nanofluids, Al_2O_3 nanofluids, ZnO nanofluids, CuO nanofluids, and pure water, in that order.
Venkateswarlu et al. (2023) [75]	CuO/EG-water and Al_2O_3/EG-water.	$0 \leq \phi \leq 0.10$	Both nanoparticles' temperatures are raised by 36.52% and 44.20% as a result of an increase in volume percent, correspondingly. Because of their unique thermophysical features, CuO:EG-water nanofluids reach their optimal temperatures 7.68% faster than Al_2O_3/EG-water nanofluids.
Kanti et al. (2024) [16]	Al_2O_3 and CuO nanofluids.	$0 \leq \phi \leq 0.005$	When compared to water alone, the 0.5% Al_2O_3-CuO Nf significantly reduced the temperature of LIB cells by 54.23% at a flowrate of 350 ml/min.
Moayedi (2025) [76]	TiO_2, CuO, Al_2O_3, Fe_3O_4, ZnO, Cu, Ag, and Graphene	$0 \leq \phi \leq 0.03$	A 0.22 K drop in maximum temperature and a 0.09 K drop in volume fraction are both possible with an improved convective heat transfer coefficient and nanofluids, respectively.
Deng et al. (2025) [77]	Al_2O_3 and TiO_2-water nanofluids.	$0 \leq \phi \leq 0.001$	Compared to water mist, the cooling time required by nanofluids was 46% shorter, taking just 11 s to bring the temperature down from its peak during thermal runaway to less than 100°C.

transitioned to the liquid phase during the testing period. Increasing duct height reduced the maximum and average temperatures of the battery cells while raising the outlet temperature of the nanofluid. At 47 min, the highest Nf HTC was observed at a duct height of 20 mm, followed closely by the 12 mm configuration. The U-value within the PCM increased consistently with duct height.

Using the FEM, Mustafa et al. [82] investigated the thermal management of a LIB coupled to a solar energy system. The battery employed a combined cooling system (CLS) incorporating both nanofluids (NFs) and nano-enhanced PCMs (N-PCMs). A bionic-shaped structure surrounded the LIB, with PCMs placed between the Nf flow channels. Water–alumina Nfs and $CaCl_2{\cdot}6H_2O$/graphene-based N-PCMs were used, where the Nf charged the N-PCMs during flow. The results showed that more heat was absorbed when N-PCMs were used instead of conventional PCMs. The addition of NPs to the N-PCMs also increased the volume percentage of melted PCM. Increasing the NF inlet velocity and adding NPs to the N-PCMs led to a rise in outlet temperature of the CLS, while simultaneously decreasing the average temperature and increasing the Nusselt number (Nu). Rapid flow acceleration enhanced N-PCM charging, thereby increasing the N-PCM melting volume fraction. Ultimately, the study concluded that a hybrid cooling system combining nanofluids and N-PCMs provides superior thermal management for LIBs, particularly under high heat generation conditions.

A cylindrical LIB with helical coolant channels was proposed by Jilte et al. [83] for improved thermal management. The study investigated the impact of four different concentrations of Al_2O_3 NPs, 0%, 2%, 5%, and 10%, in the base fluid on the efficiency of heat removal from the battery cooling system. Two types of base fluid configurations were considered: one involved PCM enclosed within a cylindrical container surrounding the battery, and the other used cooling water circulating through liquid channels connected to the outer walls of the cylinder. The research focused on three thermal management configurations: the standard PCM-WLC setup, which consisted of a cylindrical container filled with RT-42 PCM for battery cooling; the nePCM-WLC configuration, which incorporated nano-enhanced PCM into the cooling circuit; and the nePCM-LC configuration, which used nano-enhanced PCM loaded into helical liquid channels. In the nePCM-LC setup, the PCM container was equipped with channels allowing Nf circulation. The results demonstrated that the nePCM-LC configuration, utilising helical channels, outperformed the traditional TMS based on straight rectangular channels. It achieved superior heat removal from the PCM and significantly enhanced the overall cooling performance of the battery.

Using the FEM, Chen et al. [84] conducted three-dimensional simulations of a plate-type LIB TMS. This battery configuration is particularly suitable for aerospace applications, where weight is a critical factor. On either side of the battery cell was an enclosure filled with PCM, and at the centre of the PCM enclosure, a tube was embedded to circulate alumina/water Nf as part of the active cooling system. The researchers used a two-phase flow model to perform the simulation. To generate temperature contours for the system, PCM,

and coolant tube – as well as to observe the PCM melting front and the volume fraction (VFN) of molten PCM – the Nf velocity was varied from 10 to 30 mm/s, and the position of the tube inside the PCM enclosure was adjusted. The results showed that increasing the Nf velocity from 10 to 30 mm/s resulted in a 14.8% reduction in the average system temperature and an 18.9% reduction in the molten PCM volume fraction after 1200 s. The lowest average system temperature and the greatest amount of solid PCM occurred when the tube was placed 8 mm from the battery centre. In contrast, a tube distance of 11 mm produced the highest average temperature and the lowest VFN of solid PCM.

Chen et al. [85] conducted three-dimensional modelling of a plate-type LIB's TMS, incorporating both PCM and Nf flow. PCM was housed on both sides of the battery, and a channel within the PCM allowed the flow of alumina/water nanofluids. A two-phase model was employed to simulate NF flow. The number of embedded tubes within the PCM was varied from one to four, while the Nf velocity was adjusted between 10 and 30 mm/s. The study examined how the tube-to-battery distance influenced both the maximum battery temperature and the volume fraction of molten PCM (VFMPC). FEM was used to carry out the simulations. An 8 mm tube separation resulted in the highest maximum battery temperature and VFMPC, while a 5 mm gap led to the lowest maximum battery temperature and VFMPC. The increase in the number of tubes led to a decrease in VFMPC, as more heat was effectively removed. Additionally, the highest maximum battery temperature decreased over time due to continued heat dissipation. Increasing the Nf velocity also contributed to improved cooling. When the velocity was raised from 10 to 30 mm/s, the highest maximum battery temperature was reduced by 45.37% after 1200 s.

Referring to the obtained results of aluminium-nanofluids in LIBs with PCM, it can be said that a 19.5% decrease of maximum battery temperature can be attained by integrating active and passive cooling approaches in a comparison to traditional approaches, with aluminum nanofluids lowering temperatures by 15.5%. Utilising alumina nanofluids with copper foam PCM can actvely delays paraffin melting, prolonging operational time under high discharge rates. Also, blade-shaped nanoparticles in passive cooling setups can be used to reduce battery temperatures and the volume of molten PCM, while increased flow velocity can improve heat transfer coefficients. Higher duct heights were practiced to enhance thermal performance, leading to lower maximum battery temperatures. Furthermore, integrating nanofluids into PCMs can increase heat absorption and melting volume, upgrading cooling efficiency. The relevant studies showed that an optimum placement of circulation tubes within PCM enclosures can meaningfully lower the average system temperatures and rises the volume of solid PCM.

3.2.2. Carbon-nanofluid

The use of a heatsink for thermal management in LIBs was investigated by Rostami et al. [86]. The innovative heatsink design incorporated both nanofluids (NFs) and PCMs. A helical microchannel (MCH) was employed to deliver the NFs to the heatsink, which also featured a series of spiral-shaped pin fins. The microchannels were filled with a nano-enhanced PCM composed of graphene NPs. The study evaluated several parameters, including the heat transfer coefficient (HTC), the volume of molten PCM over time, the Nf outlet temperature, and the maximum and average PCM temperatures (T_M and T_A, respectively), under variable Re numbers. Simulations were carried out using the COMSOL Multiphysics software. The results indicated that, for all cases except Re = 500, the volume of molten PCM increased over time until the heatsink was fully saturated. However, when Re was equal to or greater than 500, the PCM remained solid, and the melting process ceased entirely within the heatsink. Over time, both the PCM temperature and the Nf outlet temperature increased. However, as the Reynolds number increased, the outlet temperature of the nanofluid, along with the average and maximum temperatures of the PCM (T_A and T_M), decreased. Additionally, the HTC between the PCM and the Nf showed a time-dependent and Reynolds number–dependent increase, demonstrating improved heat exchange under higher flow conditions.

3.2.3. Different types of nanofluids

The objective of the study conducted by Kiani et al. [87] was to evaluate the TMS of pouch-type LIB modules. The experimental setup involved the use of nanofluid-based cooling systems, as well as copper foam embedded with paraffin wax serving as a PCM due to its high heat storage capacity. For comparison, TMSs using only water were also tested. An inlet duct made of aluminum heat sinks was proposed to enhance heat dissipation. To simulate the high current discharge and thermal runaway conditions typically experienced by LIBs, a battery surrogate was used. Experimental results demonstrated that the nanofluid-based system significantly improved cooling efficiency. Among the various oxide-based Nf slurries tested, silver oxide (AgO) emerged as the most effective. Compared to

conventional water-based cooling systems, the use of an AgO/water Nf with a 2 vol.% concentration reduced the maximum battery temperature by 4.1 K. Additionally, the inclusion of copper foam, whether combined with PCM or not, was found to reduce the maximum battery temperature differential by 77%.

To further explore battery cooling strategies, Torregrosa et al. [88] analysed the use of NPs and nano-encapsulated PCMs. The researchers evaluated six different nano-encapsulated PCMs and five types of NPs. A battery module undergoing charging at a 4C rate was assessed, with a coolant flow rate of 2 L/min and both ambient and fluid temperatures set to 20°C. Nf concentrations ranged from 0.01% to 5%. Two key performance metrics, maximum temperature during charging and the total heat transferred to the coolant, were used to assess cooling effectiveness. The results indicated that increasing nanoparticle concentration improved both metrics. Among thirty combinations of NPs and nano-encapsulated PCMs tested, copper oxide (CuO) combined with octadecane provided the optimal balance between heat dissipation and temperature control. At 20°C, a maximum temperature reduction of 2°C was achieved using a 5 vol.% nanofluid, compared to the baseline without NPs. Additionally, this combination led to a 28% increase in total heat removed by the coolant.

Wang et al. [89] used the FEM to model a cooling system for battery packs consisting of multiple LIB cells, incorporating laminar Nf flow and PCMs. The two-phase flow model was employed to simulate the behaviour of the nanofluid, and the system included curved cooling walls. Each battery cell was encased in PCM and positioned within an elliptical housing. To evaluate the transient effects of varying design parameters, the researchers examined changes in vertical spacing between the batteries (0.7–1.1 units), horizontal spacing (0.5–1 unit), and Nf inlet size (0.5–1.5 units). Key performance metrics included battery temperature, the heat transfer coefficient (HTC), and the phase change behaviour of the PCM. To identify optimal design conditions, the results were further refined using an artificial intelligence (AI) optimisation approach. The findings revealed that the highest pressure drop, a 583% increase, occurred at the configuration with the greatest horizontal spacing, the smallest vertical spacing, and the largest NFD inlet size. The lowest maximum battery temperature was observed when the smallest NFD inlet dimension was used, in combination with the shortest horizontal and vertical distances between battery cells, resulting in a 7.15° improvement compared to other configurations. The highest HTC value (794.26 W/m^2 K) occurred when the horizontal spacing between the NFD and battery cells was maximised, even though this coincided with the lowest vertical spacing and largest NFD inlet dimensions.

The above revised studies introduced a number of facts. First, using silver oxide (AgO) can reduce the maximum battery peak temperature by 4.1 K compared to water. Second, the inclusion of copper foam can decrease the maximum battery temperature differential by 77%, improving heat dissipation. Third, copper oxide (CuO) of 5 vol.% nanofluid with octadecane can achieve a temperature reduction of 2°C besides increasing total heat removal by 28%. Fourth, optimal design configurations in a cooling system can enhance the maximum battery temperature by 7.15°C, highlighting the position of inlet size and spacing. Finally, the maximum heat transfer coefficient (794.26 W/m^2 K) was obtained with increased horizontal spacing, signigying the design difficulties.

3.2.4. Hybrid nanofluids

Al-Rashed [90] conducted a numerical analysis of a solar-powered battery pack composed of cylindrical cells. The system included a charger designed to store energy in the battery – an essential function for enabling the use of solar energy in EV. The charger also allowed for variable charging rates to accommodate different operational needs. For thermal management, a hybrid cooling approach combining nanofluids (NFs) and nano-enhanced PCMs was implemented. Simulations were performed using FEM. The results indicated that the combined use of nanofluids and nano-enhanced PCMs significantly improved heat transfer rates and reduced the time required for PCM melting and solidification. As the volume fraction of NPs (VPNPs) increased, the Nusselt number (Nu) also increased prior to the onset of the phase transition. Moreover, PCM charged through a circular cross-sectional tube demonstrated a 10.7% improvement in the freezing process. The battery temperature decreased by up to 0.5% for the circular tube configuration and by 0.37% for the elliptical tube when the VPNPs were increased. Table 2 provides a summary of published studies related to the use of nanofluids in LIBs in combination with PCM-based cooling strategies.

4. Critical analysis of LIBs with nanofluids and PCM

The evaluation of nanofluid- and PCM-based TMSs for LIBs involves a comprehensive analysis of their advantages, limitations, and operational challenges. Nanofluids enhance heat transfer, particularly when Al_2O_3–water NPs are used, achieving up to 20% improvement in thermal conductivity. This enhancement

Table 2. An immediate representation of the scientific articles linked to the nanofluids in LIBs with PCM.

The researchers (year) [reference]	Nanofluid composition	Nanofluid concentration	Results and remarks
Aluminium-nanofluids			
Mashayekhi et al. (2020) [78]	Al_2O_3-water nanofluid.	0.01 and 0.02	Using nanofluids in active and hybrid methods can lower the max. battery temperature by 15.5% and 8.5% compared to the basic case with water flow.
Kiani et al. (2020) [79]	Al_2O_3-water nanofluid.	$0 \leq \phi \leq 0.01$	Substituting Nf for water successfully delays the start of the paraffin phase transition, which in turn increases the melting time and reduces the rate of temperature increase.
Jiang et al. (2022) [80]	Al_2O_3-water nanofluid.	$0 \leq \phi \leq 0.06$	Increased velocity resulted in a 1.24°C drop in MAX and 1.53°C drop in AVG battery temperatures as well as a 0.44°C drop in output Nf temperature.
Jiang et al. (2022) [81]	Al_2O_3-water nanofluid.	$0 \leq \phi \leq 0.02$	Upon reaching 47 min, the nanofluid's highest heat transfer coefficient is noted at a height of 20 mm, with the 12 mm height of the ducts following closely after.
Mustafa et al. (2022) [82]	Al_2O_3-water nanofluid.	$0 \leq \phi \leq 0.04$	Increasing the entrance velocity of the NFs and adding NPs to the N-PCM both raise the CLS's outlet temperature. An increase in the NFs velocity lowers the average CLS temperature and increases the Nu value.
Jilte et al. (2023) [83]	Al_2O_3-water nanofluid.	$0 \leq \phi \leq 0.1$	In comparison to a BTMS based on straight rectangular channels, the nePCM-LC configuration's helical channels allow for more effective heat removal from the PCM, leading to cooler batteries.
Chen et al. (2023) [84]	Al-water nanofluid.	$0 \leq \phi \leq 0.1$	The av. temperature of the BTY drops by 14.8% and the VFN of molten PCM drops by 18.9% in 1200 s when the VNF was increased from 10 to 30 mm/s.
Chen et al. (2023) [85]	Al_2O_3-water nanofluid.	$0 \leq \phi \leq 0.01$	Reducing the maximum T-BT is the result of improving the VNF. By changing the VNF from 10 to 30 mm/s, the maximum T-BT may be reduced by 45.37% in 1200 s.
Carbon-nanofluid			
Rostami et al. (2022) [86]	Graphene nanofluid.	$0 \leq \phi \leq 0.1$	The quantity of NFs temperature at the outlet and the T-A and T-M of PCM within the heatsink are both reduced when the Re increases.
Different types of nanofluids			
Kiani et al. (2020) [87]	Al_2O_3, AgO, CuO-water nanofluid.	$0.01 \leq \phi \leq 0.04$	In a contrast against the BTMS that rely on pure water, those that use an AgO/water Nf with a 2 vol.% concentration lower the maximum temperature of the battery by 4.1 K.
Torregrosa et al. (2023) [88]	CuO, Al_2O_3, SiO2, ZnO, TiO2 nanofluids.	$0.01 \leq \phi \leq 0.05$	Compared to the scenario without NPs, a volume fraction of 5% reduces the maximum temperature by approximately 2°C.
Wang et al. (2023) [89]	Ag and MgO-water nanofluid.	$0.001 \leq \phi \leq 0.007$	While the vertical distance between the batteries and the largest NFD input dimensions was the lowest, the highest HTC (794.26 W/m^2 K) happened at the greatest horizontal distance between the NFD and batteries.
Hybrid nanofluids			
Al-Rashed (2022) [90]	Al_2O_3-CuO hybrid nanofluid.	$0 \leq \phi \leq 0.4$	Raising the volume percentage of VPNPs lowers the battery temperature by 0.37% for the elliptical tube and up to 0.5% for the circular tube.

contributes to reduced peak temperatures and improved thermal uniformity during high-discharge operations.

Hybrid systems incorporating PCMs, such as paraffin and composite materials, act as heat absorbers that delay thermal instability and extend operational safety by mitigating thermal runaway and storing latent heat. However, long-term stability is hindered by two critical issues: nanoparticle agglomeration and sedimentation, which degrade thermal performance, and increased pumping power requirements due to elevated Nf viscosity. The effectiveness of PCMs is also limited by their inherently low thermal conductivity and volumetric expansion during phase transitions. Nevertheless, performance can be improved by incorporating metal foams or graphene-based additives. Economic and environmental concerns also arise from the high cost of nanomaterials and the challenges associated with Nf disposal. At the systems level, optimisation of channel configurations, such as wavy microchannels, and balancing thermal efficiency with overall energy performance remain areas requiring further investigation. Despite these challenges, the integration of nanofluids with PCM systems offers substantial potential, including up to a 23% reduction in battery temperature and the extension of battery lifespan.

Referring to the obtained results of relevant studies of integrated nanofluids with LIBs and without phase change materials, it can be stated that the combined Al_2O_3 and CuO hybrid nanofluid in water can attain the maximum peak LIB cell temperatures reduction of 54.23% in at optimal flow rates. In this aspect, the use of optimal conditions of 1.0–2.0 vol.% of nanoparticle concentration, 0.1–0.5 m/s of flow rate can maximise the heat transfer. Furthermore, the implementation of microchannel or helical coil designs of ooling system is useful to improve surface area and heat transfer efficiency. Also, maintaining operating temperatures below 42°C during discharge is essential to secure battery safety and competence.

In the same context and relating to the outomes of relevant studies of integrated nanofluids with LIBs and with phase change materials, the combination of aluminum nanofluids and silver oxide nanofluids with nano-enhanced PCMs (such as octadecane) can attain the maximum peak temperature reduction of 19.5%. Also,

Table 3. Performance-Cost-Sustainability Trade-off framework for nanofluid-PCM systems.

Category	Cooling mechanism strength	Cost	Sustainability	Key challenges
Al_2O_3-water	Moderate (1.2–19.5% ΔT reduction)	Low-moderate	Moderate (sedimentation)	Nanoparticle stability
Hybrid (Al_2O_3-CuO)	High (up to 54.23% ΔT reduction)	High	Low (high viscosity, energy use)	Cost and pumping power
Carbon-based	High (130–135% thermal conductivity)	Very high	Moderate (recyclability issues)	Scalability and cost
PCM-metal foam	High (uniformity <2°C)	Moderate	High (reusable)	Low thermal conductivity

the opimal consitions of 1.0–5 vol.% nanoparticle concentration and 0.1–0.5 m/s of flow rate can elucidate the active cooling (optimum heat transfer) without excessive pressure drop. Then, the use of elliptical tube configurations for PCM circulation was deduced as the optimum design configuration that can attain a notable improvement in freezing processes (up to 10.7%). Also, the higher duct heights can enahnce thermal performance and enable better flow distribution.

A comparative matrix is provided in Table 3, which classifies nanofluid-PCM systems into cooling performance (such as temperature-reduction, thermal homogeneity), costs (costs of nanoparticle/material), and sustainability (environmental effect, stability). This framework would eliminate any dispute by focusing on trade-offs e.g. the Al_2O_3 -water nanofluids have good cooling effect (19.5% temperature drop) and moderate price, but have sedimentation effects whilst hybrid nanofluids (e.g. Al_2O_3-CuO) has best performance (54.23% reduction) but higher price. Such gaps noted by the matrix include the necessity of scalable, low-agglomeration nanofluids and sustainable PCM composites.

The numerical environmental indicators include GHG emissions reduction due to optimised BTMS, the life cycle assessment (LCA) data between nanofluids-PCM systems and the conventional cooling system, and the energy efficiency steps (e.g. 19.5% energy use decrease using hybrid systems). Moreover, the recyclability of the nanofluids and PCMs and the ability to reduce carbon footprint of electric vehicles (EVs). The thermal runaway risks can also be alleviated through the nanofluid-based cooling, which indirectly helps to mitigate dangerous emissions.

Table 4 depicts a comparison of the performance of nanofluid and PCM-based thermal management systems in key relevant parameter (cooling efficiency, temperature uniformity, pressure drop, or cost of these systems) and multiple differentiators that may be considered in different applications with potential application (e.g. EVs vs. grid storage):

Table 4. Comparative analysis of nanofluid and PCM-based thermal management systems for EVs and grid storage applications.

Metric	EV applications	Grid Storage applications
Cooling Efficiency	High (e.g. Al_2O_3-water nanofluids reduce peak temps by 1.2°C at 2% concentration)	Moderate (PCMs prioritise latent heat storage over rapid cooling)
Temperature Uniformity	Critical (maintained within 2° C for safety)	Less critical (larger battery packs tolerate slight variations)
Pressure Drop	Moderate (increased viscosity requires optimised channel designs)	Low (slower flow rates acceptable)
Cost	Higher (due to complex nanofluid systems)	Lower (PCMs with passive cooling are cost-effective)
Scalability	Challenging (space constraints in compact designs)	Feasible (modular PCM integration suits large-scale systems)

5. Conclusions

The current review evaluates nanofluids in conjunction with PCMs as effective strategies for enhancing the thermal management of LIBs. The key findings from the reviewed studies can be summarised as follows:

(1) Temperature peaks were reduced by 1.2°C when using Al_2O_3–water nanofluids at a 2% volume concentration, while overall cooling efficiency improved by 5–8%.
(2) Al_2O_3–CuO hybrid nanofluids achieved 54.23% greater temperature reduction compared to water alone.
(3) The lowest average battery temperatures were recorded when using 5 vol.% SiO_2 nanofluids, which reduced extreme temperatures by up to 47°C.
(4) The combination of paraffin-based PCMs with Al_2O_3 nanofluids led to a 15–20% reduction in maximum battery temperature.
(5) The thermal conductivity of nano-enhanced PCMs, such as graphene–paraffin composites, increased by 130–135%, resulting in more uniform heat distribution.
(6) The integration of serpentine microchannels with hydrophobic walls improved heat transfer capacity by up to 20%.
(7) Hybrid nanofluid–PCM systems, when combined with metal foams, maintained temperature

differentials below 2°C, effectively preventing thermal runaway.

(8) Compared to conventional water-based systems, the use of AgO/water Nf at a 2 vol.% concentration reduced maximum battery temperature by 4.1 K.
(9) Increasing the inlet velocity of nanofluids and incorporating NPs into nano-enhanced PCMs (N-PCMs) raised the outlet temperature of the combined liquid system (CLS). However, a higher NF velocity also lowered the average CLS temperature and increased the Nusselt number (Nu).
(10) Nanofluids used in active and hybrid cooling strategies reduced maximum battery temperature by 15.5% and 8.5%, respectively, compared to basic water-based systems.
(11) A 0.22 K reduction in maximum temperature and a 0.09 K reduction in molten PCM volume fraction were observed with improved convective heat transfer coefficients and the use of nanofluids.
(12) The temperatures of Al_2O_3 and CuO nanofluids increased by 36.52% and 44.20%, respectively, as a result of increased nanoparticle volume fractions. Due to their unique thermophysical properties, CuO/EG–water nanofluids reached optimal temperature levels 7.68% faster than Al_2O_3/EG–water nanofluids.
(13) The superior heat transfer characteristics of Al_2O_3–GO hybrid nanofluids make them highly effective for BTMS, even under high current discharge conditions.

6. Further enhancements and accompanying challenges

LIBs aim to enhance their power capacity and charging speed through advanced TMS that utilise nanofluids in combination with PCMs. While current advances in this area show promise, further technical improvements are needed to maximise system functionality and address existing limitations. This section analyses key areas for improvement and identifies surmountable barriers that must be overcome to enable practical deployment.

6.1. Opportunities for enhancement

(1) The use of proprietary nanoparticle mixtures, combining metal-based, oxide-based, and carbon-based NPs, can improve thermal conductivity by over 50% compared to baseline commercial coolants.
(2) Surface functionalization of NPs enhances dispersion stability, minimising long-term sedimentation during operation.
(3) Magnetic nanofluids are under development, offering thermoregulation through responsiveness to external magnetic fields.
(4) The development of nano-encapsulated PCMs with tailored phase change temperatures can better suit diverse battery operating scenarios.
(5) Incorporating graphene aerogels and metal–organic frameworks into PCM composites significantly improves thermal conductivity.
(6) The integration of porous structures into PCM storage systems helps prevent leakage while preserving maximum energy storage capacity.
(7) Predictive algorithms are being developed to enable adaptive thermal control based on variable operating parameters.
(8) The integration of multi-scale cooling approaches, combining microchannel cold plates with PCM-based passive systems, offers improved temperature regulation.
(9) Thermoresponsive materials are being explored for self-regulating cooling systems that adjust cooling intensity based on real-time thermal loads.
(10) Regarding the heating scenario, AI/ML models can improve the optimisation aspects of the cooling solutions in real-time. Magnetic nanofluids, thermoresponsive, and adaptive cooling systems have self-regulating possibilities and solid-state batteries present new thermal demands and opportunities to design their own unique TMS.

6.2. Key challenges

(1) Nanoparticle aggregation and sedimentation in nanofluids can degrade thermal performance over time.
(2) PCMs are prone to phase segregation and property degradation after repeated thermal cycles.
(3) Compatibility issues may arise between nanofluids, PCMs, and battery cell components.
(4) Nanofluids typically have higher viscosities than conventional fluids, increasing the required pumping power.
(5) Space limitations in compact battery designs make PCM integration challenging.
(6) Hybrid active–passive systems often require complex control strategies for optimal operation.

(7) The production of engineered nanofluids and advanced PCM composites remains cost-prohibitive.
(8) Achieving scalable manufacturing of uniform, stable nanofluids is still a significant challenge.
(9) The lack of standardised testing protocols for performance evaluation hinders cross-study comparisons.
(10) Some organic materials used in PCMs present flammability risks.
(11) Concerns about nanoparticle release and associated environmental impacts persist.
(12) Recycling and disposal of nano-enhanced thermal materials present logistical and environmental difficulties.

6.3. Future perspectives for overcoming challenges

(1) Develop cost-effective, environmentally friendly nanofluids with stable long-term performance.
(2) Employ advanced characterisation techniques to assess system behaviour under extended operational conditions.
(3) Design integration strategies that optimise thermal performance alongside energy density and system-level parameters.
(4) Establish standardised guidelines for nanofluid- and PCM-based battery cooling systems through collaboration with industry stakeholders.
(5) Focus on the production of environmentally friendly nanofluids that are cost effective and are more stable due to high level of surface functionalization.
(6) Some of the specific predictions are the use of magnetic nanofluids in adaptive thermal regulation in running operating conditions and the incorporation of multi-scale cooling strategies to comprise microchannel cold plates and graphene-enhanced PCMs to attain better temperature uniformity.
(7) A scalable technology of the uniform nanofluids and standardised tests should be developed to help bring about the industry adoption.

Author contributions

Farhan Lafta Rashid: Conceptualisation, Data curation, Formal analysis, Investigation, Methodology, Visualisation, Writing– original draft. Mudhar A. Al-Obaidi: Conceptualisation, Data curation, Formal analysis, Investigation, Methodology, Visualisation, Supervision, Writing review & editing. Najah M. L. Al Maimuri: Visualisation, Resources. Ali M. Ashour: Investigation, Resources. Shabbir Ahmad: Investigation, Visualisation. Arman Ameen: Formal analysis, Writing review & editing, Visualisation. Saif Ali Kadhim: Formal analysis, Investigation, Visualisation. Karrar A. Hammoodi: Formal analysis, Investigation. Wisam J. Khudhayer: Formal analysis, Resources. Ali Altaee: Formal analysis, Investigation,. All authors provided intellectual content, edited the manuscript, approved the final version for submission and agree to be accountable for all aspects of the work.

Disclosure statement

No potential conflict of interest was reported by the author(s).

Data availability statement

The authors confirm that the data supporting thefindings of this study are available within the article.

ORCID

Farhan Lafta Rashid http://orcid.org/0000-0002-7609-6585
Mudhar A. Al-Obaidi http://orcid.org/0000-0002-1713-4860
Najah M. L. Al Maimuri http://orcid.org/0000-0002-7752-4182
Shabbir Ahmad http://orcid.org/0000-0001-7152-1354
Arman Ameen http://orcid.org/0000-0002-8349-6659
Ali Altaee http://orcid.org/0000-0001-9764-3974

References

[1] Liu J, Yadav S, Salman M, et al. Review of thermal coupled battery models and parameter identification for lithium-ion battery heat generation in EV battery thermal management system. Int J Heat Mass Transf. 2024 Jan;218(1):124748. doi:10.1016/j.ijheatmasstransfer.2023.124748
[2] Hussein SS, Abid AJ, Obed AA, et al. Boosting Li-Ion battery pack lifespan with active on-load balancing. J Tech. 2023;5(4):77–87. doi:10.51173/jt.v5i4.1328
[3] Zaidan M, Hasan G, Al-Obaidi M. Comparative study between a battery and super-capacitor of an electrical energy storage system for a traditional vehicle. Gazi Univ J Sci. 2022;35(4):1405–1415. doi:10.35378/gujs.969972
[4] Feng XN, Sun J, Ouyang MG, et al. Characterization of penetration induced thermal runaway propagation process within a large for-mat lithium ion battery module. J Power Sources. 2015;275:261–273. doi:10.1016/j.jpowsour.2014.11.017
[5] Togun H, Aljibori HSS, Biswas N, et al. A critical review on the efficient cooling strategy of batteries of electric vehicles: advances, challenges, future perspectives. Renewable Sustainable Energy Rev. 2024;203:114732. doi:10.1016/j.rser.2024.114732

[6] Liu HR, Wen C, Yuen ACY, et al. A novel thermal management system for battery packs in hybrid electrical vehicles utilising waste heat recovery. Int J Heat Mass Transf. 2022;195:123199. doi:10.1016/j.ijheatmasstransfer.2022.123199
[7] Xu PH, Liu BL, Hu XY, et al. State-of-charge estimation for lithium-ion batteries based on fuzzy information granulation and asymmetric Gaussian membership function. IEEE Trans Ind Electron. 2022;69:7.
[8] Alshammari A, Al-Obaidi MA, Staggs J. Modelling and simulation of thermal runaway phenomenon in lithium-ion batteries. Asia-Pac J Chem Eng. 2024;19(2):e3004. doi:10.1002/apj.3004
[9] Zhang LW, Zhao P, Xu M, et al. Computational identification of the safety regime of Li-ion battery thermal runaway. Appl Energy. 2020;261:114440. doi:10.1016/j.apenergy.2019.114440
[10] Gungor S, Cetkin E, Lorente S. Canopy-to-canopy liquid cooling for the ther-mal management of lithium-ion batteries, a constructal approach. Int J Heat Mass Transf. 2022;182:121918. doi:10.1016/j.ijheatmasstransfer.2021.121918
[11] Lai YX, Wu WX, Chen K, et al. A compact and lightweight liquid– cooled thermal management solution for cylindrical lithium-ion power battery pack. Int J Heat Mass Transf. 2019;144:118581. doi:10.1016/j.ijheatmasstransfer.2019.118581
[12] Mo X, Zhi H, Xiao Y, et al. Topology optimisation of cooling plates for battery thermal management. Int J Heat Mass Transf. 2021;178:121612. doi:10.1016/j.ijheatmasstransfer.2021.121612
[13] Zhao D, An C, Jia Z, et al. Structure optimisation of liquid-cooled plate for electric vehicle lithium-ion power batteries. Int J Therm Sci. 2024 Jan;195(1):108614. doi:10.1016/j.ijthermalsci.2023.108614
[14] Rashid FL, Mohammed HI, Dulaimi A, et al. Analysis of heat transfer in various cavity geometries with and without nano-enhanced phase change material: a review. Energy Rep. 2023;10:3757–3779. doi:10.1016/j.egyr.2023.10.036
[15] Zhong J-F, Sedeh SN, Lv Y-P, et al. Investigation of ferro-nanofluid flow within a porous ribbed microchannel heat sink using single-phase and two-phase approaches in the presence of constant magnetic field. Powder Technol. 2021;387:251–260. doi:10.1016/j.powtec.2021.04.033
[16] Kanti PK, Yang ESJ, Wanatasanappan VV, et al. Impact of hybrid and mono nanofluids on the cooling performance of lithium-ion batteries: experimental and machine learning insights. J Energy Storage. 2024 Nov;101(Part A):113613. doi:10.1016/j.est.2024.113613
[17] Cai LR, Li Z, Zhang SS, et al. Safer lithium-ion battery anode based on Ti 3 C 2 Tz MXene with thermal safety mechanistic elucidation. Chem Eng J. 2021;419:129387. doi:10.1016/j.cej.2021.129387
[18] Chen C, Tang Y, Ma Y, et al. Research on the influence of thermal radiation of cell phone system on the structure and safety of lithium-ion battery. J Power Sources. 2024 Apr;598(1):234160. doi:10.1016/j.jpowsour.2024.234160
[19] Napa N, Agrawal MK, Tamma B. Development of electro-thermal model for prismatic Lithium-ion cell subjected to electric vehicle drive cycle using converging fluid channel. Int J Therm Sci. 2024 May;199(1):108936. doi:10.1016/j.ijthermalsci.2024.108936
[20] Li W, Li Y, Garg A, et al. Enhancing real-time degradation prediction of lithium- ion battery: a digital twin framework with CNN-LSTM-attention model. Energy. 2024 Jan;286(1):129681. doi:10.1016/j.energy.2023.129681
[21] Yao J, Chang Z, Han T, et al. Semi-supervised adversarial deep learning for capacity estimation of battery energy storage systems. Energy. 2024 Mar;294(2):130882. doi:10.1016/j.energy.2024.130882
[22] Bahrami D, Nadooshan AA, Bayareh M. Effect of non-uniform magnetic field on mixing index of a sinusoidal micromixer. Korean J Chem Eng. 2022 Jan;45(1):1–12.
[23] Sun H, Xiang X, Wang X, et al. Advanced photo-rechargeable lithium-and zinc-ion batteries: progress and prospect. J Power Sources. 2024 Apr;598(1):234204. doi:10.1016/j.jpowsour.2024.234204
[24] Xiang P, Jiang K, Wang J, et al. Evaluation of LCOH of conventional technology, energy storage coupled solar PV electrolysis, and HTGR in China. Appl Energy. 2024 Jan;353(1):122086. doi:10.1016/j.apenergy.2023.122086
[25] Gasmelseed A, Ismael MA, Said MA, et al. Thermal management strategies for lithium-ion batteries in electric vehicles: a comprehensive review of nanofluid-based battery thermal management systems. Res Eng. 2024;24:103339. doi:10.1016/j.rineng.2024.103339
[26] Can A, Selimefendigil F, Öztop HF. A review on soft computing and nanofluid applications for battery thermal management. J Energy Storage. 2022;53:105214. doi:10.1016/j.est.2022.105214
[27] Yang L, Zhou F, Sun L, et al. Thermal management of lithium-ion batteries with nanofluids and nano-phase change materials: a review. J Power Sources. 2022;539:231605. doi:10.1016/j.jpowsour.2022.231605
[28] Sefidan AM, Sojoudi A, Saha SC. Nanofluid-based cooling of cylindrical lithium-ion battery packs employing forced air flow. Int J Therm Sci. 2017;117:44–58. doi:10.1016/j.ijthermalsci.2017.03.006
[29] Sarchami A, Tousi M, Kiani M, et al. A novel nanofluid cooling system for modular lithium-ion battery thermal management based on wavy/stair channels. Int J Therm Sci. 2022;182:107823. doi:10.1016/j.ijthermalsci.2022.107823
[30] Sarchami A, Najafi M, Imam A, et al. Experimental study of thermal management system for cylindrical Li-ion battery pack based on nanofluid cooling and copper sheath. Int J Therm Sci. 2022;171:107244. doi:10.1016/j.ijthermalsci.2021.107244
[31] Liu S, Liu Y, Gu H, et al. Experimental study of the cooling performance of γ-Al2O3/heat transfer fluid nanofluid for power batteries. J Energy Storage. 2023;72(Part C):108476. doi:10.1016/j.est.2023.108476
[32] Wang D, Abdullah MM, Alizadeh A, et al. Numerical investigation of parallel microchannels on a battery pack in the buildings with the aim of cooling by applying nanofluid-optimisation in channel numbers. J Taiwan Inst Chem Eng. 2023;148:104894. doi:10.1016/j.jtice.2023.104894
[33] Anqi AE. Numerical investigation of heat transfer and entropy generation in serpentine microchannel on the battery cooling plate using hydrophobic wall and nanofluid. J Energy Storage. 2023;66:106548. doi:10.1016/j.est.2022.106548
[34] Ouyang T, Liu B, Wang C, et al. Novel hybrid thermal management system for preventing Li-ion battery thermal

runaway using nanofluids cooling. Int J Heat Mass Transfer. 2023;201(Part 2):123652. doi:10.1016/j.ijheatmasstransfer.2022.123652

[35] Jha P, Hussain M, Khan MK. Numerical evaluation of nanofluid-based indirect liquid cooling of a Li-ion battery pack using equivalent circuit model under static and dynamic loading conditions. Int Commun Heat Mass Transfer. 2024;159(Part A):108079. doi:10.1016/j.icheatmasstransfer.2024.108079

[36] Banerjee R, Nidhul K. Thermal management of high-discharge lithium-ion prismatic cells using various dielectric nanofluid-based novel immersion cooling design. J Therm Anal Calorim. 2025;150(6):4833–4849. doi:10.1007/s10973-025-14040-y

[37] Wu F, Rao Z. The lattice Boltzmann investigation of natural convection for nanofluid based battery thermal management. Appl Therm Eng. 2017;115:659–669. doi:10.1016/j.applthermaleng.2016.12.139

[38] Zhao L, Jasim DJ, Alizadeh A, et al. Offering a channel for cooling three lithium-ion battery packs with water/Cu nanofluid: an exergoeconomic analysis. Ain Shams Eng J. 2024;15(7):102788. doi:10.1016/j.asej.2024.102788

[39] Qawasmeh BR, Alrbai M, George S. Cooling of lithium-ion battery using PCM passive and semipassive thermal system immersed in nanofluid. Energy Explor Exploit. 2024;43(2):776–799. doi:10.1177/01445987241310003

[40] Chen M, Li J. Nanofluid-based pulsating heat pipe for thermal management of lithium-ion batteries for electric vehicles. J Energy Storage. 2020;32:101715. doi:10.1016/j.est.2020.101715

[41] Wiriyasart S, Hommalee C, Sirikasemsuk S, et al. Thermal management system with nanofluids for electric vehicle battery cooling modules. Case Stud Therm Eng. 2020;18:100583. doi:10.1016/j.csite.2020.100583

[42] Ziad Saghir M, Rahman MM, Bicer Y. Investigation of channel materials toward better cooling lithium-ion batteries in the presence of nanofluid and pin-fins. Int J Thermofluids. 2023;18:100349. doi:10.1016/j.ijft.2023.100349

[43] Saghir MZ, Bicer Y. Thermohydraulic performance of ammonia, isopropanol, water and nanofluids as cooling fluid for lithium-ion 1C and 3C rating batteries. Int J Thermofluids. 2023;20:100433. doi:10.1016/j.ijft.2023.100433

[44] Yang X, Zhao Z, Liu Y, et al. Simulation of nanofluid-cooled lithium-ion battery during charging: a battery connected to a solar cell. Int J Mech Sci. 2021;212:106836. doi:10.1016/j.ijmecsci.2021.106836

[45] Aberoumand S, Woodfield P, Shi G, et al. Thermo-electro-rheological behaviour of vanadium electrolyte-based electrochemical graphene oxide nanofluid designed for redox flow battery. J Mol Liq. 2021;338:116860. doi:10.1016/j.molliq.2021.116860

[46] Zhou Z, Lv Y, Qu J, et al. Performance evaluation of hybrid oscillating heat pipe with carbon nanotube nanofluids for electric vehicle battery cooling. Appl Therm Eng. 2021;196:117300. doi:10.1016/j.applthermaleng.2021.117300

[47] Kim J, Park H. Enhanced mass transfer in nanofluid electrolytes for aqueous flow batteries: the mechanism of nanoparticles as catalysts for redox reactions. J Energy Storage. 2021;38:102529. doi:10.1016/j.est.2021.102529

[48] Aberoumand S, Dubal D, Woodfield P, et al. Enhancement in vanadium redox flow battery performance using reduced graphene oxide nanofluid electrolyte. J Energy Storage. 2023;72(Part B):108343. doi:10.1016/j.est.2023.108343

[49] Mitra A, Kumar R, Singh DK. Thermal management of lithium-ion batteries using carbon-based nanofluid flowing through different flow channel configurations. J Power Sources. 2023;555:232351. doi:10.1016/j.jpowsour.2022.232351

[50] Rana S, Zahid H, Kumar R, et al. Lithium-ion battery thermal management system using MWCNT-based nanofluid flowing through parallel distributed channels: an experimental investigation. J Energy Storage. 2024;81:110372. doi:10.1016/j.est.2023.110372

[51] Tousi M, Sarchami A, Kiani M, et al. Numerical study of novel liquid-cooled thermal management system for cylindrical Li-ion battery packs under high discharge rate based on AgO nanofluid and copper sheath. J Energy Storage. 2021;41:102910. doi:10.1016/j.est.2021.102910

[52] Jahanbakhshi A, Nadooshan AA, Bayareh M. Cooling of a lithium-ion battery using microchannel heatsink with wavy microtubes in the presence of nanofluid. J Energy Storage. 2022;49:104128. doi:10.1016/j.est.2022.104128

[53] Azizi Z, Barzegarian R, Behvandi M. Design-expert aided thermohydraulic assessment of a nanofluid-cooled cylindrical microchannel heat sink: possible application for thermal management of electric vehicle batteries. Sustainable Energy Technol Assess. 2022;50:101876. doi:10.1016/j.seta.2021.101876

[54] Rahmani E, Fattahi A, Panahi E, et al. Thermal management improvement for a pack of cylindrical batteries using nanofluids and topological modifications. J Power Sources. 2023;564:232876. doi:10.1016/j.jpowsour.2023.232876

[55] Sarchami A, Tousi M, Darab M, et al. Novel AgO-based nanofluid for efficient thermal management of 21700-type lithium-ion battery. Sustainable Energy Technol Assess. 2024;70:103934. doi:10.1016/j.seta.2024.103934

[56] Yetik O, Karakoc TH. Thermal and electrical analysis of batteries in electric aircraft using nanofluids. J Energy Storage. 2022;52(Part B):104853. doi:10.1016/j.est.2022.104853

[57] Dilbaz F, Selimefendigil F, Öztop HF. Lithium-ion battery module performance improvements by using nanodiamond-FE_3O_4 water/ethylene glycol hybrid nanofluid and fins. J Therm Anal Calorim. 2022;147:10625–10635. doi:10.1007/s10973-022-11269-9

[58] Yetik O, Morali U, Karakoc TH. A numerical study of thermal management of lithium-ion battery with nanofluid. Energy. 2023;284:129295. doi:10.1016/j.energy.2023.129295

[59] Jongpluempiti J, Vengsungnle P, Poojeera S, et al. Thermal profile analysis of 18650 Li-ion battery module with embedded copper foam in the nanofluid cooling jacket. Case Stud Chem Environ Eng. 2025;11:101208. doi:10.1016/j.cscee.2025.101208

[60] Alqaed S, Mustafa J, Almehmadi FA, et al. The effect of using non-Newtonian nanofluid on pressure drop and heat transfer in a capillary cooling system connected to a pouch lithium-ion battery connected to a Solar System. J Power Sources. 2022;539:231540. doi:10.1016/j.jpowsour.2022.231540

[61] Alnaqi AA. Numerical analysis of pressure drop and heat transfer of a non-Newtonian nanofluids in a Li-ion battery thermal management system (BTMS) using bionic geometries. J Energy Storage. 2022;45:103670. doi:10.1016/j.est.2021.103670

[62] Hasan HA, Togun H, Abed AM, et al. Efficient cooling system for lithium-ion battery cells by using different concentrations of nanoparticles of SiO2-water: a numerical investigation. Symmetry (Basel). 2023;15:640. doi:10.3390/sym15030640

[63] Hasan HA, Togun H, Abed AM, et al. Cooling lithium-ion batteries with silicon dioxide -water nanofluid: CFD analysis. Renewable Sustainable Energy Rev. 2025;208:115007. doi:10.1016/j.rser.2024.115007

[64] Venkateswarlu B, Chavan S, Joo SW, et al. Impact of hybrid nanofluids on thermal management of cylindrical battery modules: a numerical study. J Energy Storage. 2024;99(Part A):113266. doi:10.1016/j.est.2024.113266

[65] Thawkar V, Dhoble AS, Shewalkar AG. Enhanced thermal management of electric vehicle lithium-ion batteries with Al_2O_3–MWCNT–ethylene glycol hybrid nanofluid-based helical coiled pulsating heat pipe (HC-PHP). J Therm Anal Calorim. 2024;149:6241–6251. doi:10.1007/s10973-024-13076-w

[66] Sheikholeslami M, Esmaeili Z, Momayez L. Numerical analysis of lithium-ion battery performance with new mini-channel configurations implementing hybrid nanofluid. J Taiwan Inst Chem Eng. 2025;171:106074. doi:10.1016/j.jtice.2025.106074

[67] Selvarajoo K, Wanatasanappan VV, Luon NY, et al. Cooling performance of 18650 lithium-ion battery module using Al2O3-GO hybrid and mono nanofluids: A numerical study with experimental validation. Case Stud Thermal Eng. 2025;68:105842. doi:10.1016/j.csite.2025.105842

[68] Kumar K, Sarkar J, Mondal SS. Analysis of ternary hybrid nanofluid in microchannel-cooled cylindrical Li-ion battery pack using multi-scale multi-domain framework. Appl Energy. 2024;355:122241. doi:10.1016/j.apenergy.2023.122241

[69] Liu Q, Liu F, Liu S, et al. Improved performance of Li-ion battery thermal management system by ternary hybrid nanofluid. J Energy Storage. 2025;109:115234. doi:10.1016/j.est.2024.115234

[70] Mondal B, Lopez CF, Mukherjee PP. Exploring the efficacy of nanofluids for lithium-ion battery thermal management. Int J Heat Mass Transfer. 2017;112:779–794. doi:10.1016/j.ijheatmasstransfer.2017.04.130

[71] Liu H, Chika E, Zhao J. Investigation into the effectiveness of nanofluids on the mini-channel thermal management for high power lithium ion battery. Appl Therm Eng. 2018;142:511–523. doi:10.1016/j.applthermaleng.2018.07.037

[72] Kiani M, Omiddezyani S, Nejad AM, et al. Novel hybrid thermal management for Li-ion batteries with nanofluid cooling in the presence of alternating magnetic field: An experimental study. Case Stud Therm Eng. 2021;28:101539. doi:10.1016/j.csite.2021.101539

[73] Liao G, Wang W, Zhang F, et al. Thermal performance of lithium-ion battery thermal management system based on nanofluid. Appl Therm Eng. 2022;216:118997. doi:10.1016/j.applthermaleng.2022.118997

[74] Hasan HA, Togun H, Abed AM, et al. Numerical investigation on cooling cylindrical lithium-ion-battery by using different types of nanofluids in an innovative cooling system. Case Stud Therm Eng. 2023;49:103097. doi:10.1016/j.csite.2023.103097

[75] Venkateswarlu B, Chavan S, Joo SW, et al. A numerical study on heat transfer performance using nanofluids in liquid cooling for cylindrical battery modules. J Mol Liq. 2023;391(Part A):123257. doi:10.1016/j.molliq.2023.123257

[76] Moayedi H. Exploring the potential of various nanofluids for thermal management of a lithium-ion battery. Appl Therm Eng. 2025;261:125177. doi:10.1016/j.applthermaleng.2024.125177

[77] Deng J, Hu Z, Chen J, et al. The enhanced cooling effect and critical control capability of nanofluids on suppressing thermal runaway of lithium-ion batteries. J Energy Storage. 2025;106:114733. doi:10.1016/j.est.2024.114733

[78] Mashayekhi M, Houshfar E, Ashjaee M. Development of hybrid cooling method with PCM and Al2O3 nanofluid in aluminium minichannels using heat source model of Li-ion batteries. Appl Therm Eng. 2020;178:115543. doi:10.1016/j.applthermaleng.2020.115543

[79] Kiani M, Ansari M, Arshadi AA, et al. Hybrid thermal management of lithium-ion batteries using nanofluid, metal foam, and phase change material: an integrated numerical–experimental approach. J Therm Anal Calorim. 2020;141:1703–1715. doi:10.1007/s10973-020-09403-6

[80] Jiang Y, Wang X, Mahmoud MZ, et al. A study of nanoparticle shape in water/alumina/boehmite nanofluid flow in the thermal management of a lithium-ion battery under the presence of phase-change materials. J Power Sources. 2022;539:231522. doi:10.1016/j.jpowsour.2022.231522

[81] Jiang Y, Smaisim GF, Mahmoud MZ, et al. Simultaneous numerical investigation of the passive use of phase-change materials and the active use of a nanofluid inside a rectangular duct in the thermal management of lithium-ion batteries. J Power Sources. 2022;541:231610. doi:10.1016/j.jpowsour.2022.231610

[82] Mustafa J, Alqaed S, Almehmadi FA, et al. Effect of simultaneous use of water-alumina nanofluid and phase change nanomaterial in a lithium-ion battery with a specific geometry connected Solar System. J Power Sources. 2022;539:231570. doi:10.1016/j.jpowsour.2022.231570

[83] Jilte R, Afzal A, Ağbulut Ü, et al. Battery thermal management of a novel helical channeled cylindrical Li-ion battery with nanofluid and hybrid nanoparticle-enhanced phase change material. Int J Heat Mass Transfer. 2023;216:124547. doi:10.1016/j.ijheatmasstransfer.2023.124547

[84] Chen H, Zhou W, Yuan Y, et al. Effect of tube location on the temperature of plate lithium-ion battery applicable in the aerospace industry in the presence of two-phase nanofluid flow inside a channel placed in phase change material. Eng Anal Boundary Elem. 2023;150:624–635. doi:10.1016/j.enganabound.2023.02.051

[85] Chen H, Zhou W, Yuan Y, et al. Impact of the number of tubes containing nanofluid flow on the melting and freezing of phase change materials in the thermal management of plate lithium-ion batteries. Eng Anal

Boundary Elem. 2023;151:464–472. doi:10.1016/j.enganabound.2023.03.029

[86] Rostami S, Nadooshan AA, Raisi A, et al. Effect of using a heatsink with nanofluid flow and phase change material on thermal management of plate lithium-ion battery. J Energy Storage. 2022;52(Part A):104686. doi:10.1016/j.est.2022.104686

[87] Kiani M, Omiddezyani S, Houshfar E, et al. Lithium-ion battery thermal management system with Al2O3/AgO/CuO nanofluids and phase change material. Appl Therm Eng. 2020;180:115840. doi:10.1016/j.applthermaleng.2020.115840

[88] Torregrosa AJ, Broatch A, Olmeda P, et al. Analysis of the improvement of a lithium-ion battery module cooling system employing nanofluid and nano encapsulated phase change materials by means of a lumped electro-thermal model. J Energy Storage. 2023;70:107995. doi:10.1016/j.est.2023.107995

[89] Wang D, Ali MA, Alizadeh A, et al. A numerical investigation of a two-phase nanofluid flow with phase change materials in the thermal management of lithium batteries and use of machine learning in the optimisation of the horizontal and vertical distances between batteries. Case Stud Therm Eng. 2023;41:102582. doi:10.1016/j.csite.2022.102582

[90] Al-Rashed AAAA. Thermal management of lithium-ion batteries with simultaneous use of hybrid nanofluid and nano-enhanced phase change material: a numerical study. J Energy Storage. 2022;46:103730. doi:10.1016/j.est.2021.103730